学位論文(要約)

Nonlinear wave dynamics associated with tidal dissipation in the ocean interior

(海洋内部領域での潮汐散逸に関わる非線形波動力学の研究)

平成 28 年 12 月 博士 (理学) 申請

東京大学大学院理学系研究科

地球惑星科学専攻

大貫 陽平

Abstract

The baroclinic tide, a kind of oceanic internal waves generated by a barotropic tidal flow over bottom topography, is regarded as the most significant energy source in the deep ocean. Since the dissipation of internal waves causes vertical water mixing that controls the overturning circulation of the ocean, detection of the global distribution of tidal dissipation rates is a major concern in physical oceanography. In the last decades, it has been reported that the nonlinear resonant interactions among internal waves effectively enhance the energy dissipation of baroclinic tides in the mid-latitude ocean. Even today, however, such nonlinear wave dynamics is insufficiently understood. This thesis discusses the qualitative and quantitative aspects of resonant interactions in the ocean.

Among various resonant interactions, the most important one is *parametric subharmonic instability* (PSI). In PSI, two small-scale waves with nearly opposite wave vectors are spontaneously enhanced in a large-scale wave train. While a number of numerical studies have coped with this phenomenon, physical mechanism of PSI remains obscure. In this study, PSI is redefined as a kind of parametric instability where *two disturbance waves propagating in opposite directions compose beats of velocity vectors locked with the phase of background waves resulting in successive advection of background momentum causing self-acceleration of disturbances*. This interpretation is visually presented.

More quantitative aspects of resonant interactions are investigated based on a theory of statistical physics. In general, a widely used statistical method for resonant interaction processes is the so-called *kinetic equation*, which describes long-term evolution of an energy spectrum

in a continuous medium. In some cases, however, the kinetic equation bankrupts or offers an unrealistic prediction. Especially for PSI, the growth rate of disturbance energy estimated from the kinetic equation does not agree with the result of a simple dynamic theory. This problem is successfully solved in this thesis. It is pointed out that the implicit assumption adopted to derive the kinetic equation gets invalid in an unsteady process. Introducing a generalized statistical theory, we derive a simple solution which reconciles the existing two types of studies. This new method is valid even when considering a baroclinic tide with weak phase modulation, which has not been discussed in the previous studies. Our theory also implies that the kinetic equation is valid in a steady state as far as the nonlinearity is sufficiently weak, which serves as the theoretical foundation of the theme that follows.

In the real ocean, it can be supposed that the energy generation and loss of the baroclinic tides are balanced in a steady state. Although a direct numerical simulation offers a good estimates of the generation of baroclinic tidal energy, the loss of baroclinic tidal energy depends on adjustable parameters. A proper scheme is desired to reproduce the energy loss of the baroclinic tides in numerical models. For this purpose, we utilize a new expression of the kinetic equation to formulate the attenuation rate of baroclinic tides interacting with the background wave field. Using a standard energy spectrum and the geographical data, we obtain global distribution of the attenuation rates of baroclinic tidal energy. As the main result, rapid attenuation of the tidal energy at the mid-latitudes where PSI most efficiently works is successfully reproduced. In this latitudinal band, ocean depth and density structure control the zonal variation of the attenuation rate, which can be quantified using the equivalent depth of each mode. To discuss the vertical distribution of the interaction intensity, the expression of the kinetic equation is heuristically decomposed into a vertical integration form and its integrand is analyzed. It is shown that strong stratification near the surface concentrates the generation of small-scale waves in the upper ocean, especially for the lowest-mode barolcinic tide. A series of results suggest that ongoing parameters in the conventional ocean models

need to be replaced by more reliable ones.

Overall, the theoretical basis and the numerical results in this thesis will serve as a milestone for the future study of tidal dissipation in the ocean.

Contents

Chapter 1

General introduction

1.1 Tides and ocean circulation

Periodic tidal forcing exerted by the gravity of the sun and moon extracts the rotational energy from the earth, causing up-and-down motion of the ocean surface. Summing up all the tidal constituents, the total energy directly excited from the tidal forcing is about 3.7 TW (3.7×10^{12} Joule per second) in the global ocean (Munk and Wunsch, 1998; Garrett, 2003). Although a large part of energy locally dissipates near the coast or in the ocean bottom boundary layer, some energy is converted into oceanic internal motions, called "baroclinic tides". Generation processes of baroclinic tides in the open ocean have been qualitatively and quantitatively investigated in the past decades (Garrett and Kunze, 2007). Thanks to the development of recent numerical ocean models and computational power, one can directly simulate the generation and propagation of baroclinic tides (Niwa and Hibiya, 2004, 2011; Shriver et al., 2012). Using a high resolution numerical model, Niwa and Hibiya (2014) estimated that the total energy of baroclinic tides generated in the global ocean amounts to about 1.2 TW (Fig. 1.1). Global patterns of surface displacements associated with baroclinic tides are also detected from satellite altimeters (Ray and Zaron, 2016; Zhao et al., 2016).

Despite the endeavors of innumerable researchers, how and where the baroclinic tidal energy dissipates in the ocean remain unknown even today.

Tidal dissipation in the ocean is related to the global ocean circulation. In general, energy dissipation in a stratified fluid causes vertical water mixing, associated with the energy conversion from kinetic energy into potential energy (Osborn, 1980; Huang, 2009). This process is crucial to overturn the dense water spreading from polar region to the global deep ocean (Munk, 1966). It is widely known that numerically reproduced deep ocean states badly depend on the vertical diffusivity in the model (Bryan, 1987; Tsujino et al., 2000). An accurate estimates of energy dissipation rates in the ocean is one of the main concerns of modern physical oceanography.

1.2 Tidal dissipation caused by nonlinear resonances

One key process for the energy dissipation of baroclinic tides is the nonlinear resonance among internal waves. The first formulation of wave-wave interaction theory for oceanic internal waves dates back to 1960's. Despite the long history of study, the significant progress was made in this century. It was revealed that, the intensity of interaction between baroclinic tides and the surrounding wave components highly depends on the local Coriolis parameter, resulting in the remarkable latitudinal dependence of energy dissipation rates. Following the first observational report (Fig. 1.2) in Hibiya and Nagasawa (2004), a large number of numerical, observational, and theoretical studies have been made for the wave-wave interaction processes linked with the tidal energy dissipation in the ocean.

The most well-known character of nonlinear resonance for internal waves is "resonant condition". In general, three wave components with wave vectors $\boldsymbol{k}_1, \boldsymbol{k}_2, \boldsymbol{k}_3$ and the corre-

sponding frequencies $\omega_1, \omega_2, \omega_3$ can interact with each other if the conditions

$$\boldsymbol{k}_1 \pm \boldsymbol{k}_2 \pm \boldsymbol{k}_3 = 0 \tag{1.1a}$$

$$\omega_1 \pm \omega_2 \pm \omega_3 = 0 \tag{1.1b}$$

are satisfied. McComas and Bretherton (1977) pointed out that major interaction among oceanic internal waves can be classified into three types, called, induced diffusion (ID), elastic scattering (ES), and parametric subharmonic instability (PSI), which are described in Fig. 1.3. Numerical studies such as Hibiya et al. (2002) have shown that PSI plays a key role for the energy dissipation of baroclinic tides. In order for PSI to occur in a wave train of a baroclinic tide with frequency ω_T, other two waves with ω_1, ω_2 need to satisfy

$$\omega_1 + \omega_2 = \omega_T. \tag{1.2}$$

Taking account of the dispersion relation of inertia-gravity waves, PSI occurs only equatorward of the latitude where half the tidal frequency coincides with the local inertial frequency. As for the principal lunar semi-diurnal constituent (M_2 Tide), 28.89° is the so-called *critical latitude*. Observational and numerical studies tend to suggest that PSI most effectively acts near the critical latitude, with the abrupt switch off at the higher latitudes and rather smooth relaxation toward the lower latitudes (Hibiya and Nagasawa, 2004; Furuichi et al., 2005; MacKinnon and Winters, 2005; Kunze et al., 2006; Hibiya et al., 2007; Simmons, 2008; Hazewinkel and Winters, 2011; Qiu et al., 2012). A simple empirical formula in Hibiya et al. (2006) suggests that the global distribution of tidal dissipation rate is strongly controlled by the resonant interaction processes in the ocean (Fig. 1.4).

1.3 Short review of theoretical studies

Energy transfer rate in wave vector space caused by wave-wave interaction in the ocean has been investigated in substantial literature until now, reviews of which can be seen in

Olbers (1983); Müller et al. (1986); Polzin and Lvov (2011). The standard model for weak nonlinear interactions among dispersive waves is called a "kinetic equation", which extracts only resonant interactions from all the possible combination of wave vectors and describes the long-term behavior of an energy spectrum (Hasselmann, 1962, 1966; Hasselmann and Saffman, 1967; Zakharov et al., 1992; Nazarenko, 2011). The kinetic equation significantly reduces the fundamental equation so that it is useful to calculate the energy transfer rate in wave vector space. Kinetic equations act only in weakly nonlinear systems where interaction time is sufficiently longer than an intrinsic period of each component.

Using a kinetic equation, nonlinear interactions of oceanic internal waves had been rigorously investigated until 1980's. In this era, however, resonant interaction theories were not regarded to be useful to deal with the tidal dissipation processes from two reasons. First, small-scale internal waves which controll local energy dissipation rates are *too intense* to be treated with the resonant interaction theory (McComas, 1977; Holloway, 1980, 1982). Second, on the contrary, the internal wave spectrum was regarded to be *too weak* to attenuate the large-scale baroclinic tides (Olbers and Pomphrey, 1981). These statements have been reversed by a series of numerical experiments in Hibiya et al. (1996, 1998, 2002), where PSI is redefined as the key process for the tidal dissipation in the ocean interior.

Why did the classical studies overlook the significance of PSI? Young et al. (2008), (hereafter Y08) tackled this question. They reformulated the PSI process with an asymptotic expansion and estimated the growth rate of disturbance energy in a monochromatic wave train of a baroclinic tide. It is true that their estimates well agree with the results of numerical experiments. They made, however, serious misconception for the interpretation of past studies.

1.3.1 Time scales of PSI

Y08 reasoned that the *random phase assumption* adopted in the kinetic equation made PSI seem insignificant. This argument is not correct. If a kinetic equation is applied to the problem treated in Y08, the growth rate *diverges to infinity*. Olbers and Pomphrey (1981), using a kinetic equation, had calculated not the growth time of disturbance energy, but the attenuation time of tidal energy in an oceanic internal wave spectrum. These two time scales are confused in Y08.

Another discussion can be seen in Polzin and Lvov (2011). They showed that the growth rate of disturbance energy in baroclinic tides with a broadband energy spectrum can be derived with the kinetic equation. However, their formulation still bankrupts in the limit of a monochromatic plane wave. Reasonable explanation for this confliction has never been provided.

1.3.2 Beyond the kinetic equation

Two types of theoretical approach is well known for non-weak nonlinear interaction processes of internal waves. One is ray-tracing method, where variation of the wave vector and amplitude of each wave packet is calculated along the wave trajectory in physical and wave vector space. This method is suited to describe waves in random and inhomogeneous media and serves as the theoretical basis of the practical parameterization of water mixing in the ocean interior; the energy dissipation rates are estimated from fine-scale data (Henyey et al., 1986; Polzin et al., 1995; Ijichi and Hibiya, 2015, 2016). However, the ray-tracing method can not cope with resonant interactions.

Another approach is called *direct interaction approximation* (DIA), which was originally developed for homogeneous isotropic turbulence in Kraichnan (1959). Carnevale and Fred-

eriksen (1983), Dewitt and Wright (1982, 1984), and Yokoyama (2011) discussed the DIA approach to internal wave dynamics and showed that the kinetic equation is an approximate form of the DIA equation. More generally speaking, statistical theories for classical media, including DIA and the kinetic equation, are related to quantum field theory. Martin-Siggia-Rose (MSR) formalism (Martin et al., 1973) is the most general method for the statistical dynamics of classical systems.

MSR formalism is the *exact* theory. Using some approximation, the DIA equation and the kinetic equation are systematically derived from MSR formalism. In order to solve the problems discussed in 1.3.1, the derivation process of the kinetic equation need to be reconsidered.

1.3.3 Toward the application to numerical ocean models

As for the attenuation time of baroclinic tidal energy, Eden et al. (2014) (hereafter E14) reflected on Olbers and Pomphrey (1981) and stated that the past calculation had underestimated the resonant processes of baroclinic tides due to the computational restriction. Their new study, however, still offers suspicious results. The global distribution of the resonant coupling intensity between baroclinic tides and background waves estimated in E14 failed to show the rapid attenuation of baroclinic tidal energy near the critical latitudes (Fig. 1.5). It may be because of their rough treatment of the background energy spectrum. Another problematic issue in E14 is that their formulation is based on the 3-dimensional Fourier expansion. In general, far-propagating baroclinic tides are too large to be treated as vertically propagating sinusoidal waves (Fig. 1.6).

Recent numerical studies such as Oka and Niwa (2013) discuss that the attenuation rate of baroclinic tides is the key uncertainty factor for the global circulation model. In order to obtain the accurate energy dissipation rates from a result of tidal simulation, we need more reliable estimates of attenuation rates of baroclinic tides, using new formulation and

calculation methods for the nonlinear interaction processes of internal waves.

1.4 Overview of this thesis

In this study, qualitative and quantitative aspects of nonlinear interactions between baroclinic tides and surrounding waves are investigated from the theoretical view point. In the next chapter, visual clarification of the excitation mechanism of disturbance waves in baroclinic tides are suggested using concepts of ”beats”. In Chapter 3, based on the general theories for statistical dynamics, existing conflicting studies for the growth rate of parametric instability are reconciled from a unified view point. In Chapter 4, using the expression derived from statistical theories, the attenuation rate of baroclinic tidal energy is calculated and its geography is clarified. The final chapter summarizes this study and discusses the possible practical use of the results.

General statistical theories for linear and nonlinear waves are systematically introduced and developed in the appendices. In Appendix A, mathematical description of linear waves in inhomogeneous media is discussed based on the concept of pseudo-differential operator. In Appendix B, general formalism of statistical dynamics for interacting waves is reviewed and rearranged. In Appendix C, a theoretical model of oceanic internal motion is established. Appendix D describes other complementary issues.

インターネット公表に関する同意が
得られなかったため非公表

Fig. 1.1 Numerically estimated global distribution of energy conversion rates from barotropic to baroclinic tides for the sum of the four major tidal constituents, averaged within each $2.5^\circ \times 2.5^\circ$ grid area. From Niwa and Hibiya (2014).

インターネット公表に関する同意が
得られなかったため非公表

Fig. 1.2 Estimated value of diapycnal diffusivity averaged over a depth range of 950 - 1450m at each location of field observation, using eXpendable Current Profiler (XCP). Colors denote model-predicted energy of semidiurnal internal tide vertically-integrated at each location of field observation. Remarkable latitudinal dependence of vertical diffusivity is presumably due to the occurrence of parametric subharmonic instability. From Hibiya and Nagasawa (2004).

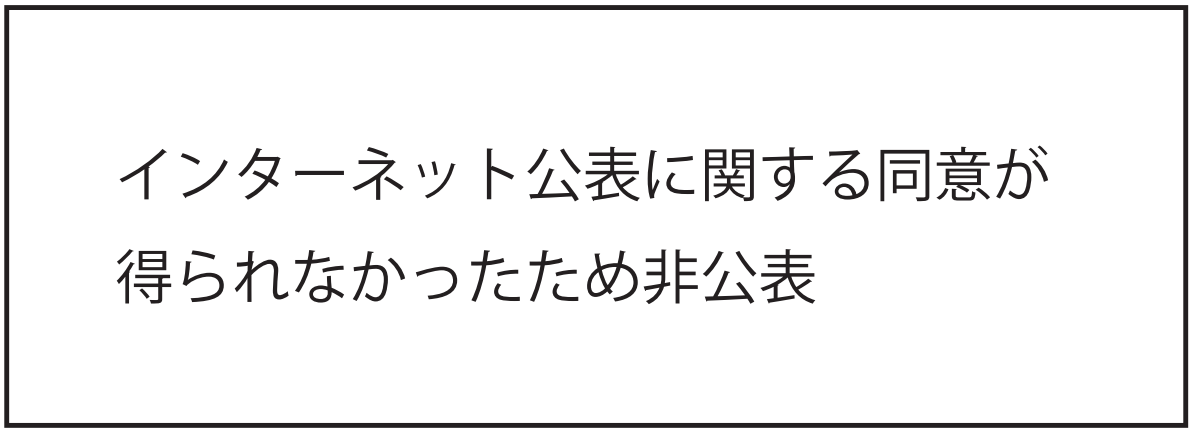

Fig. 1.3 Representation of the characteristics of typical class of triads (a)induced diffusion (b)elastic scattering (c)parametric subharmonic instability. From McComas and Bretherton (1977).

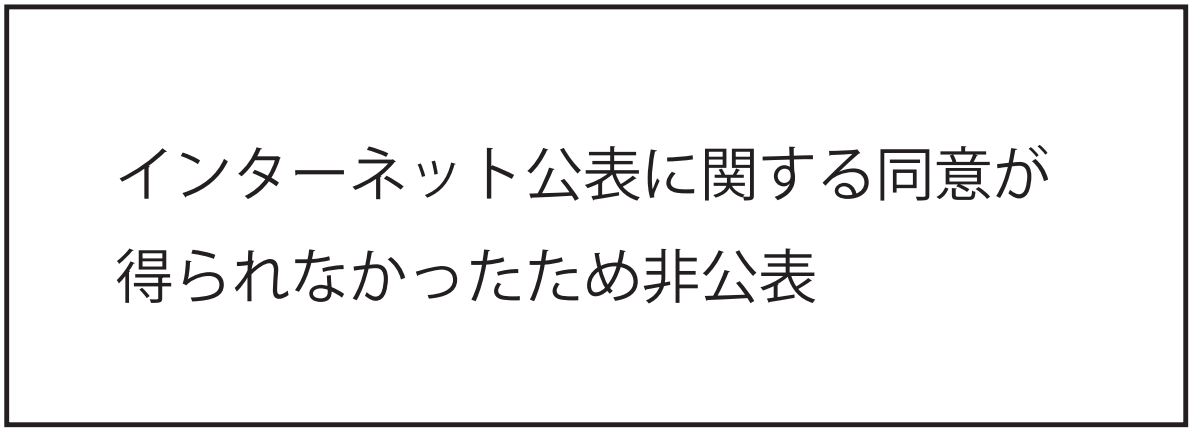

Fig. 1.4 Global distribution of the diapycnal diffusivity averaged over a depth range of 950 - 1450 m calculated by incorporating the numerically-predicted baroclinic tidal energy at each longitude and latitude into an empirical formula which reflects the effect of resonant interaction processes. From Hibiya et al. (2006).

インターネット公表に関する同意が
得られなかったため非公表

Fig. 1.5 Coupling intensity α $(10^{-6}\mathrm{s\,m^{-3}})$ of the 1st-mode M_2 baroclinic tides with background wave spectra, estimated in Eden and Olbers (2014). The attenuation rate of baroclinic tidal energy is represented as $\nu = \alpha \int E_c dz$, where E_c is the energy density of the background waves.

インターネット公表に関する同意が
得られなかったため非公表

Fig. 1.6 Model-predicted cross-sectional snapshot along 21.5°N of (a)vertical displacement and (b)horizontal velocity, excited by the tidal motion. It can be perceived that vertical 1st-mode structure is composed in far-propagating baroclinic tides. From Niwa and Hibiya (2004).

Chapter 2

Basic mechanism of PSI

2.1 Introduction

Parametric subharmonic instability (PSI) is known as the key mechanism for tidal dissipation in the mid-latitude ocean. PSI is, as its name represents, a kind of parametric instability, where a periodic motion gets unstable and subharmonic disturbances are exponentially enhanced. McComas and Bretherton (1977) detected that PSI plays a major role for the energy balance of the internal wave spectrum in the ocean. They also characterized its property that *two waves of nearly opposite wave numbers and nearly equal frequencies resonate with a much smaller wave number with almost twice the frequency* (Fig. 1.3a). Namely, the resonant conditions (1.1) are rewritten as

$$\boldsymbol{k}_3 = \boldsymbol{k}_1 + \boldsymbol{k}_2, \quad |\boldsymbol{k}_3| \ll |\boldsymbol{k}_1|, |\boldsymbol{k}_2| \tag{2.1a}$$

$$\omega_3 = \omega_1 + \omega_2, \quad \omega_3/2 \sim \omega_1, \omega_2. \tag{2.1b}$$

for PSI.

Bispectrum analysis of a numerically reproduced oceanic internal wave field interacting with baroclinic tides (Furuichi et al., 2005) suggests that the property (2.1) does hold for the

tidal component $(\boldsymbol{k}_3, \omega_3)$ and other interacting disturbance components $(\boldsymbol{k}_1, \omega_1), (\boldsymbol{k}_2, \omega_2)$. Although a large number of numerical and theoretical studies for PSI (e.g. MacKinnon and Winters (2005), Young et al. (2008)) have been done, the physical interpretation of the resonant conditions (2.1) remain obscure. Above all, how do the waves with much different scales can interact with each other?

In this chapter, the basic mechanism of PSI is clarified and a simple interpretation of the resonant conditions (2.1) is suggested. Mysterious scale separation of baroclinic tides and disturbance waves can be easily explained using the concept of *beats*. It can be said that PSI is a kind of parametric instability where *two disturbance waves propagating in opposite directions compose beats of velocity vectors locked with the phase of background waves resulting in successive advection of background momentum causing self-acceleration of disturbances*. Visualization of this property will be shown as follows.

2.2 Concept of beats

As is well known, when two sound waves with slightly different frequencies are interfered, one can hear a periodic variation of volume of sound. This phenomenon is called *beats*. As for the example of sound waves, beats can be explained with a simple expression

$$\cos\omega_1 t + \cos\omega_2 t = 2\underbrace{\cos\left(\frac{\omega_1+\omega_2}{2}t\right)}_{\text{fine waves}}\underbrace{\cos\left(\frac{\omega_1-\omega_2}{2}t\right)}_{\text{envelopes}}. \tag{2.2}$$

Then the frequency of up and down volume (beat frequency) can be expressed as $\Delta\omega = |\omega_1 - \omega_2|$, which corresponds to the frequency of peak-trough variation of envelopes of rapidly oscillating fine waves.

Now the concept of beats is extended to spatially propagating waves. A caution is needed here. Different from the 0-dimensional case, we have to take account of the direction of wave vectors for propagating waves. One usual case is two waves with slightly different

frequencies propagating in the *same* direction. In this case, the envelopes of fine waves propagate with the intrinsic group $\boldsymbol{c}_g(\boldsymbol{k})$, prescribed by the nature of the medium.

Another interesting case is when two waves with slightly different frequencies are propagating in *opposite* directions. This situation can be expressed as

$$\begin{aligned}&\cos\left(k_1 x+\omega_1 t\right)+\cos\left(k_2 x-\omega_2 t\right)\\ =&2\underbrace{\cos\left(\frac{k_1+k_2}{2}x+\frac{\omega_1-\omega_2}{2}t\right)}_{\text{fine waves}}\underbrace{\cos\left(\frac{k_1-k_2}{2}x+\frac{\omega_1+\omega_2}{2}t\right)}_{\text{envelopes}},\end{aligned} \tag{2.3}$$

where wavenumbers $k_1 \sim k_2$ and frequencies $\omega_1 \sim \omega_2$ are all taken as positive. In this case, one can observe that the envelopes of the waves seem to propagate with the phase velocity

$$c=\frac{\omega_2+\omega_1}{k_2-k_1}, \tag{2.4}$$

an example of which is described in Fig. 2.1. It should be emphasized that, different from the previous case, the propagation velocity of envelopes (2.4) does not coincide with the phase velocity nor the group velocity of component waves. In wavenumber-frequency space, we can see that the velocity (2.4) corresponds to the slope of a line which connects two points on different branches of dispersion curves (Fig. 2.2). Hence even for non-dispersive waves, one can compose various propagating speed of envelopes. In this study, envelopes composed in this way are defined as *beats*.

Although the expression (2.3) is for 1-dimensional waves, the concept of beats can be extended to more general cases. The spatial structure of beats composed of two wave vectors $\boldsymbol{k}_1 \sim \boldsymbol{k}_2$ is characterized with $\boldsymbol{k}_1 - \boldsymbol{k}_2$. From this property, we can see that the triad condition (2.1a) represents the situation where one large-scale wave $\boldsymbol{k}_3$ and beats composed of two waves $\boldsymbol{k}_1, \boldsymbol{k}_2$ possess the same spatial structure. If the frequency condition (2.1b) is also satisfied, the large-scale wave and the beats are kept in phase with time.

Then, how are the disturbance waves excited when their phases are locked to the background wave? Answer to this question depends on the specific situations. As for PSI near

the critical latitudes, it can be explained using the concepts of *flow acceleration caused by background convergence/shear*, which will be introduced in the next section.

2.3 Flow acceleration caused by background convergence/shear

We consider the equations of momentum, continuity and buoyancy in a three-dimensional rotating stratified fluid under the Boussinesq approximation;

$$\frac{\partial \boldsymbol{u}}{\partial t} + \boldsymbol{u} \cdot \nabla \boldsymbol{u} + f \boldsymbol{e}_z \times \boldsymbol{u} = -\nabla p + b \boldsymbol{e}_z, \tag{2.5a}$$

$$\nabla \cdot \boldsymbol{u} = 0 \tag{2.5b}$$

$$\frac{\partial b}{\partial t} + \boldsymbol{u} \cdot \nabla b + wN^2 = 0, \tag{2.5c}$$

where variables $\boldsymbol{u} = (u, v, w), b, p$ represent velocity, buoyancy and pressure divided by density, respectively. Constants f and N represent the inertial and buoyancy frequencies, with $N \gg f$ assumed.

Separate variables into the already-known background components $\boldsymbol{U} = (U, V, W), B, P$, which are supposed to be the exact solution of the basic equation (2.5), and infinitesimal disturbances $\boldsymbol{u}' = (u', v', w'), b', p'$. Then the time evolution of disturbances is written as

$$\frac{\partial \boldsymbol{u}'}{\partial t} + \boldsymbol{U} \cdot \nabla \boldsymbol{u}' + \boldsymbol{u}' \cdot \nabla \boldsymbol{U} + f \boldsymbol{e}_z \times \boldsymbol{u}' = -\nabla p' + b' \boldsymbol{e}_z, \tag{2.6a}$$

$$\nabla \cdot \boldsymbol{u}' = 0 \tag{2.6b}$$

$$\frac{\partial b'}{\partial t} + \boldsymbol{U} \cdot \nabla b' + \boldsymbol{u}' \cdot \nabla B + w' N^2 = 0. \tag{2.6c}$$

Multiplying (2.6a) by $\boldsymbol{u}'$ and (2.6c) by b'/N^2 and summing them up, we obtain the disturbance energy equation,

$$\frac{\partial E}{\partial t} + \nabla \cdot \boldsymbol{F} + G = 0, \tag{2.7}$$

with

$$E = \frac{1}{2}\left(u'^2 + v'^2 + w'^2 + \frac{b'^2}{N^2}\right) \tag{2.8a}$$

$$\boldsymbol{F} = p'\boldsymbol{u}' + E\boldsymbol{U} \tag{2.8b}$$

$$G = \boldsymbol{u}' \cdot (\boldsymbol{u}' \cdot \nabla)\,\boldsymbol{U} + \frac{b'}{N^2}\,(\boldsymbol{u}' \cdot \nabla)\,B, \tag{2.8c}$$

where $\boldsymbol{F}$ represents the energy flux and G represents the energy production caused by the background field. We can see that the spatial gradient of background components causes production of the disturbance energy.

Now we further assume that the aspect ratio of disturbance motions is much small, namely,

$$u', v' \gg w', \frac{b'}{N}. \tag{2.9}$$

Then the dominant factors in the energy production rate (2.8c) is

$$G \sim u'^2\frac{\partial U}{\partial x} + v'^2\frac{\partial V}{\partial y} + u'v'\frac{\partial U}{\partial y} + u'v'\frac{\partial V}{\partial x}. \tag{2.10}$$

The physical interpretation of (2.10) can be given as follows. At first, the horizontal equations of motion in (2.6) are expressed as

$$\frac{\partial u'}{\partial t} + u'\frac{\partial U}{\partial x} + v'\frac{\partial U}{\partial y} = (\text{other terms}) \tag{2.11a}$$

$$\frac{\partial v'}{\partial t} + u'\frac{\partial V}{\partial x} + v'\frac{\partial V}{\partial y} = (\text{other terms}), \tag{2.11b}$$

where terms representing the horizontal advection of background momentum are specified. From these equations, we can see two types of acceleration effects;

i). The convergence of the background flow causes the acceleration of the disturbance flow in the convergence direction (Fig. 2.3a). In other words, $\partial|u'|/\partial t \geq 0$ (or $\partial|v'|/\partial t \geq 0$) occurs when $\partial U/\partial x < 0$ (or $\partial V/\partial y < 0$).

ii). The shear of the background flow causes the acceleration of the fluctuating flow obliquely crossing the background shear layers (Fig. 2.3b). In other words, $\partial|u'|/\partial t \geq 0$ (or $\partial|v'|/\partial t \geq 0$) occurs when $u'v'\partial U/\partial y < 0$ (or $u'v'\partial V/\partial x < 0$).

It should be noted that if the direction of the background flow in Fig. 2.3(a,b) is reversed, disturbances are subject to deceleration, as is described in Fig. 2.3(c,d).

As for PSI near the critical latitudes, the convergence and shear of the background semidiurnal baroclinic tidal flow causes the steady acceleration of near-inertial disturbances, which will be examined in the next section.

2.4 PSI in baroclinic tides

2.4.1 Basic solutions

Let the background components $\boldsymbol{U}(\boldsymbol{x},t), B(\boldsymbol{x},t)$ introduced in the previous section represent baroclinic tides. Although the exact solution of equations (2.5) is difficult to obtain, a natural assumption

$$\frac{U^*T^*}{L^*} \equiv \epsilon \ll 1, \tag{2.12}$$

where T^*, L^*, U^* are the characteristic scales of time, length and velocity, yields the approximate solution of equations (2.5) as

$$(u,v,w,b,p)^T = \sum_{\boldsymbol{k}} (\tilde{u}_{\boldsymbol{k}}, \tilde{v}_{\boldsymbol{k}}, \tilde{w}_{\boldsymbol{k}}, \tilde{b}_{\boldsymbol{k}}, \tilde{p}_{\boldsymbol{k}})^T e^{i(\boldsymbol{k}\cdot\boldsymbol{x}-\omega t)} + c.c. + O(\epsilon) \tag{2.13}$$

with the polarization relation

$$\tilde{u}_{\boldsymbol{k}} = \frac{k\omega + ilf}{\omega^2 - f^2} a_{\boldsymbol{k}} \tag{2.14a}$$

$$\tilde{v}_{\boldsymbol{k}} = \frac{l\omega - ikf}{\omega^2 - f^2} a_{\boldsymbol{k}} \tag{2.14b}$$

$$\tilde{w}_{\boldsymbol{k}} = -\frac{(k^2 + l^2)\omega}{m(\omega^2 - f^2)} a_{\boldsymbol{k}} \tag{2.14c}$$

$$\tilde{b}_{\boldsymbol{k}} = \frac{i(k^2 + l^2)N^2}{m(\omega^2 - f^2)} a_{\boldsymbol{k}} \tag{2.14d}$$

$$\tilde{p}_{\boldsymbol{k}} = a_{\boldsymbol{k}}. \tag{2.14e}$$

and the dispersion relation

$$\omega = \sqrt{\frac{N^2(k^2 + l^2) + f^2 m^2}{k^2 + l^2 + m^2}}. \tag{2.15}$$

If we regard the tidal components as a monochromatic wave train with wave vector and frequency $(\boldsymbol{k}_T, \omega_T)$ in an infinite domain, $O(\epsilon)$ term in (2.13) vanishes, and hence strict stability analysis can be done for (2.6) based on the Floquet theory (for its general framework, see Sonmor and Klaassen (1997)). As is well known, in the lowest approximation, an unstable solution is written in the form of

$$(u', v', w', b', p')^T \sim \boldsymbol{q}_1 e^{i(k_1 x + l_1 y + m_1 z - \omega_1 t)} + \boldsymbol{q}_2 e^{i(k_2 x + l_2 y + m_2 z + \omega_2 t)} + c.c. \tag{2.16}$$

where $\boldsymbol{k}_1 = (k_1, l_1, m_1), \boldsymbol{k}_2 = (k_2, l_2, m_2)$ and ω_1, ω_2 satisfy the resonant conditions

$$\boldsymbol{k}_1 - \boldsymbol{k}_2 = \boldsymbol{k}_T, \quad \omega_1 + \omega_2 = \omega_T. \tag{2.17}$$

The imaginary part of an eigenvalue ω_1 represents the growth rate of disturbances corresponding to an eigenvector ($\boldsymbol{q}_1$,$\boldsymbol{q}_2$). It is expected that, because the amplitude of the background wave is assumed to be sufficiently small, $\boldsymbol{q}_1$,$\boldsymbol{q}_2$ and $\mathrm{Re}(\omega_1)$, $\mathrm{Re}(\omega_2)$ are well approximated by the basic solutions (2.14) and (2.15).

When we take account of the bottom and surface boundaries, the most simple solution for a baroclinic tide is represented in the normal mode form, where vertically symmetrical components are superimposed;

$$(U,V,W,B,P)^T = (\tilde{u}_{\boldsymbol{k}_T},\tilde{v}_{\boldsymbol{k}_T},\tilde{w}_{\boldsymbol{k}_T},\tilde{b}_{\boldsymbol{k}_T},\tilde{p}_{\boldsymbol{k}_T})^T e^{i(k_T x+l_T y+m_T z-\omega t)} + c.c. \\ + (m_T \to -m_T) + O(\epsilon). \tag{2.18}$$

Even in this case, numerical experiments (e.g. Furuichi et al. (2005)) show that a pair of mode waves gets unstable. Namely, we can suppose an unstable solution of (2.6) as

$$(u',v',w',b',p')^T \sim \boldsymbol{q}_1 e^{i(k_1 x+l_1 y+m_1 z-\omega_1 t)} + \boldsymbol{q}_2 e^{i(k_2 x+l_2 y+m_2 z+\omega_2 t)} + c.c. \\ + (m_1 \to -m_1) + (m_2 \to -m_2) \tag{2.19}$$

again with the conditions (2.17). Without loss of generality, $l_T = 0$ is taken so that the baroclinic tides are propagating in the x-z plane.

Here we consider a special situation where the tidal frequency is slightly larger than twice the local inertial frequency ($\omega_T \gtrsim 2f$), wave vectors of disturbances are much larger than that of baroclinic tides (i.e. (2.1) is satisfied) and $l_1, l_2 = 0$. It is noted that these conditions are not essential but intended to make explanation simple.

2.4.2 Flow field

The flow fields corresponding to the baroclinic tide and the disturbance waves described in (2.18) and (2.19) are visualized in Fig. 2.4: (a) represents the semidiurnal baroclinic tidal flow field projected on the vertical two-dimensional plane, (b) and (c) represent those associated with the near-inertial waves with slightly different wave vectors $\boldsymbol{k}_1, \boldsymbol{k}_2$ with the condition $\boldsymbol{k}_1 - \boldsymbol{k}_2 = \boldsymbol{k}_T$ propagating in opposite directions, and (d) represents the superposition of (b) and (c). In Fig. 2.4(d), wave groups of maximum velocity regions, namely *near-inertial beats*, become visible and propagate with a phase velocity of $(\omega_1 + \omega_2)/(k_1 - k_2)$ in light

of the discussion in Section 2.2. Comparing Fig. 2.4 (a) and (d), convergence and divergence areas in (a) correspond to the maximum and minimum velocity regions in (d) respectively. It follows that the acceleration effect of convergence exceeds the deceleration effect of divergence so that the net energy production of disturbances results. The additional condition $\omega_1 + \omega_2 = \omega_T$ ensures that the areas of convergence of the semidiurnal baroclinic tidal flow and the near-inertial beats are continuously coupled so that efficient energy transfer from the background semidiurnal tidal flow to near-inertial waves takes place.

Figure 2.5 depicts a vertical profile of horizontal velocity vectors of near-inertial disturbances. Envelopes of velocity vectors construct double helix while their component waves rapidly oscillate in the vertical direction. The rotating frequency of envelopes is written as

$$\omega_E = \frac{\omega_1 + \omega_2}{2} = \frac{\omega_T}{2}, \tag{2.20}$$

which is the notable feature of parametric excitation.

2.4.3 Parametric excitation

Figure 2.6 is a top view of a flow field in some local area, where the horizontal direction of the envelopes of velocity vectors, as is defined in Fig. 2.5, and the background semidiurnal tidal flow around them are represented as green and blue arrows. Time evolution for two tidal periods, namely 24 hours, is depicted. At 0H and 12H, because the envelopes of disturbances are along the convergence direction of the background flow, acceleration occurs by the effect of convergence, corresponding to $u'\partial U/\partial x$ in (2.11a). At 3H, 9H, 15H, and 21H, because the envelopes of disturbances obliquely cross the background shear layer, acceleration occurs by the effect of shear, corresponding to $u'\partial V/\partial x$ in (2.11b). At 6H and 18H, because the envelopes are normal to the divergent direction, they escape deceleration. Accordingly, summing up over 24 hours, net acceleration of disturbances occurs.

It should be emphasized that the frequency property (2.20) is the necessary condition for

the steady acceleration of disturbances. Similar situations can be seen in more simple systems. Pumping a playground swing by periodically standing and squatting to increase the size of the swing's oscillations is a typical example. This type of phenomena is called *parametric excitation*, which is generally characterized with periodically-varying parameter whose frequency matches with some integer multiple of intrinsic frequency of a system. As for PSI near the critical latitudes, horizontal convergence/shear of background waves acts as the time-varying parameter whose frequency matches with twice the rotation frequency of the envelopes of disturbances (*not* the frequency of component waves!).

2.4.4 More general cases

The consideration above is restricted to the vertical two-dimensional case ($l = 0$). Some modifications will be needed to discuss three-dimensional cases. Besides, leaving the critical latitudes toward the equator, waves with more broadband frequency get unstable. Then, as can be inferred from (2.14), vertical velocity w' and buoyancy b' become important. Hence all the energy production terms in (2.8c) need to be considered to discuss the specific mechanism of PSI.

In such general situations, it can still be said that beats composed of disturbance waves with half the frequency of baroclinic tides get unstable. The concept of beats is widely useful to link complicated wave-wave interaction processes to simple parametric excitation.

2.5 Conclusions

Parametric subharmonic instability is a kind of resonant interaction processes in the oceanic internal wave field, which transfers energy from baroclinic tides to small-scale waves. In this chapter, an intuitive image of its mechanism is presented based on a combination of simple concepts such as beats and parametric excitation without adhering to a strict mathematical

formula. It has been shown that beats are created by a superposition of two small-scale near-inertial waves with slightly different wave vectors propagating in opposite directions. When the resulting beats have the peak-to-peak length and the phase velocity equal to the wavelength and the phase velocity of the large-scale baroclinic tidal flow, respectively, they are resonantly coupled with each other so that near-inertial waves are *intermittently* accelerated under the effects of convergence and shear of the background baroclinic tides.

One key result in this chapter is that the energy production of disturbances is localized in some depth. As is apparent in Fig. 2.4, the 1st-mode baroclinic tides in constant stratification produces disturbance waves most efficiently near the surface or the bottom. In the real ocean with general stratification, the problem becomes more complicated, which will be discussed in Chapter 4.

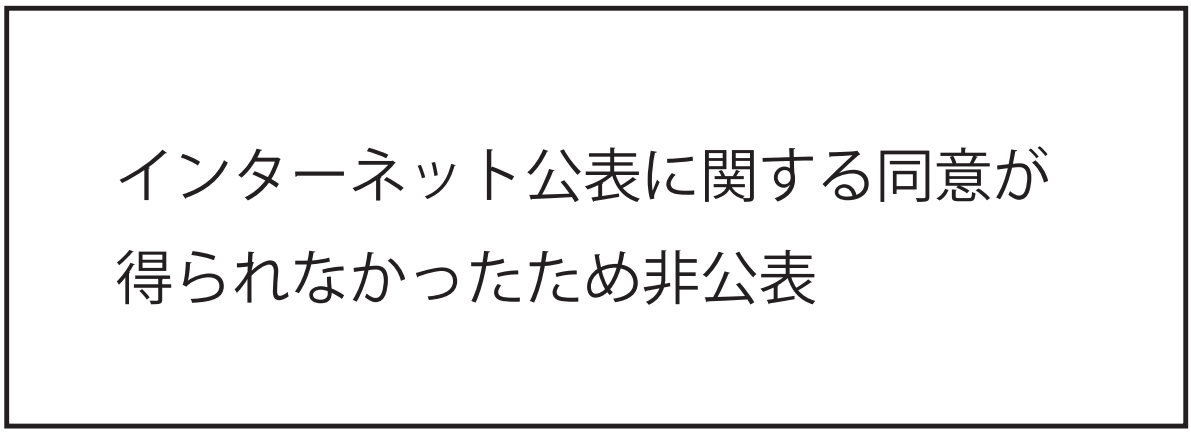

Fig. 2.1 (a)Two sinusoidal waves with slightly different wavenumbers k_1, k_2 and frequencies ω_1, ω_2 propagating in opposite directions. (b)Combining two waves produces large-scale envelopes, i.e. beats, with a large phase velocity. The resulting beats have peak-to-peak length of $2\pi/(k_1 - k_2)$ and a phase velocity of $(\omega_1 + \omega_2)/(k_1 - k_2)$.

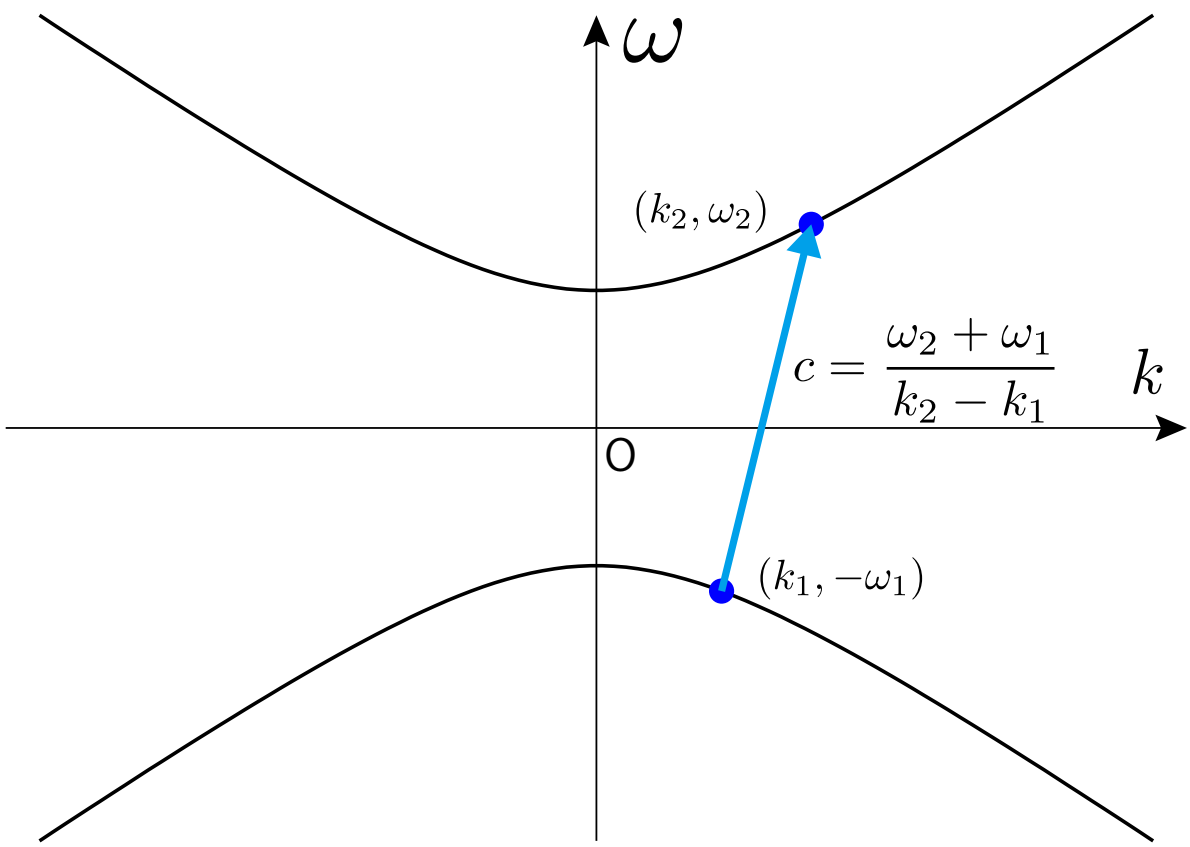

Fig. 2.2 The propagation velocity of beats is defined as the slope of a line (blue arrow) which connects two points on the different branches of dispersion curves (black curves) in the wavenumber-frequency space.

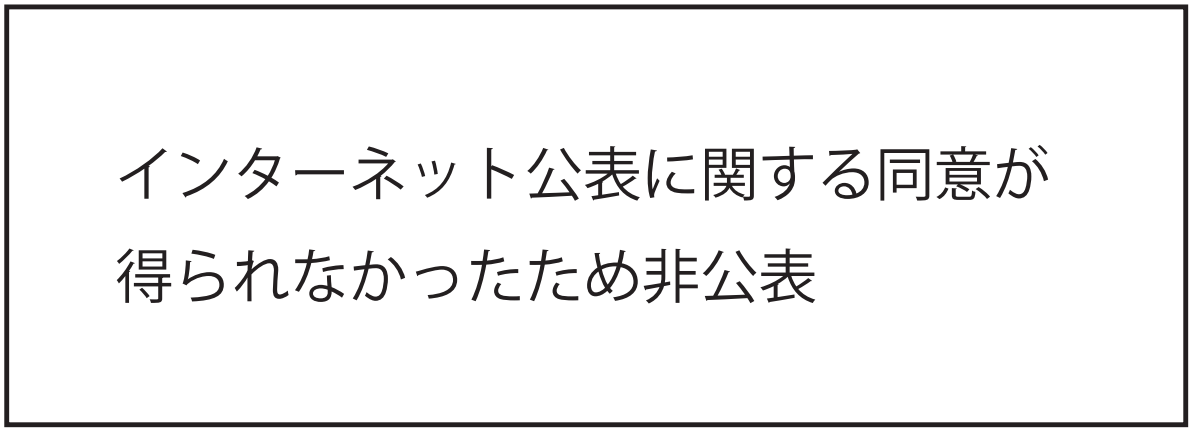

Fig. 2.3 (a)Convergence of the background flow (blue) causes the acceleration of the fluctuating flow (green) in the convergence direction and (b)shear of the background flow (blue) causes the acceleration of the fluctuating flow (green) obliquely crossing the background shear layer. (c) and (d) are the other situations where the fluctuating flow (green) are decelerated by the divergence or shear of the background flow (blue).

インターネット公表に関する同意が
得られなかったため非公表

Fig. 2.4 (a)Vertical cross section of the 1st-vertical-mode baroclinic tidal flow. The areas of horizontal convergence and divergence are colored with green and red, respectively. (b)Horizontal velocity u of near-inertial waves with wave vector $\boldsymbol{k}_1$. Blue (red) areas represent a flow directed to the the right (left). (c)As in (b) but for the near-inertial waves with wave vector $\boldsymbol{k}_2$, slightly different from $\boldsymbol{k}_1$. (d)Near-inertial beats resulting from the superposition of (b) and (c). The areas of convergence of the baroclinic tidal flow in (a) and the near-inertial beats in (d) are continuously coupled.

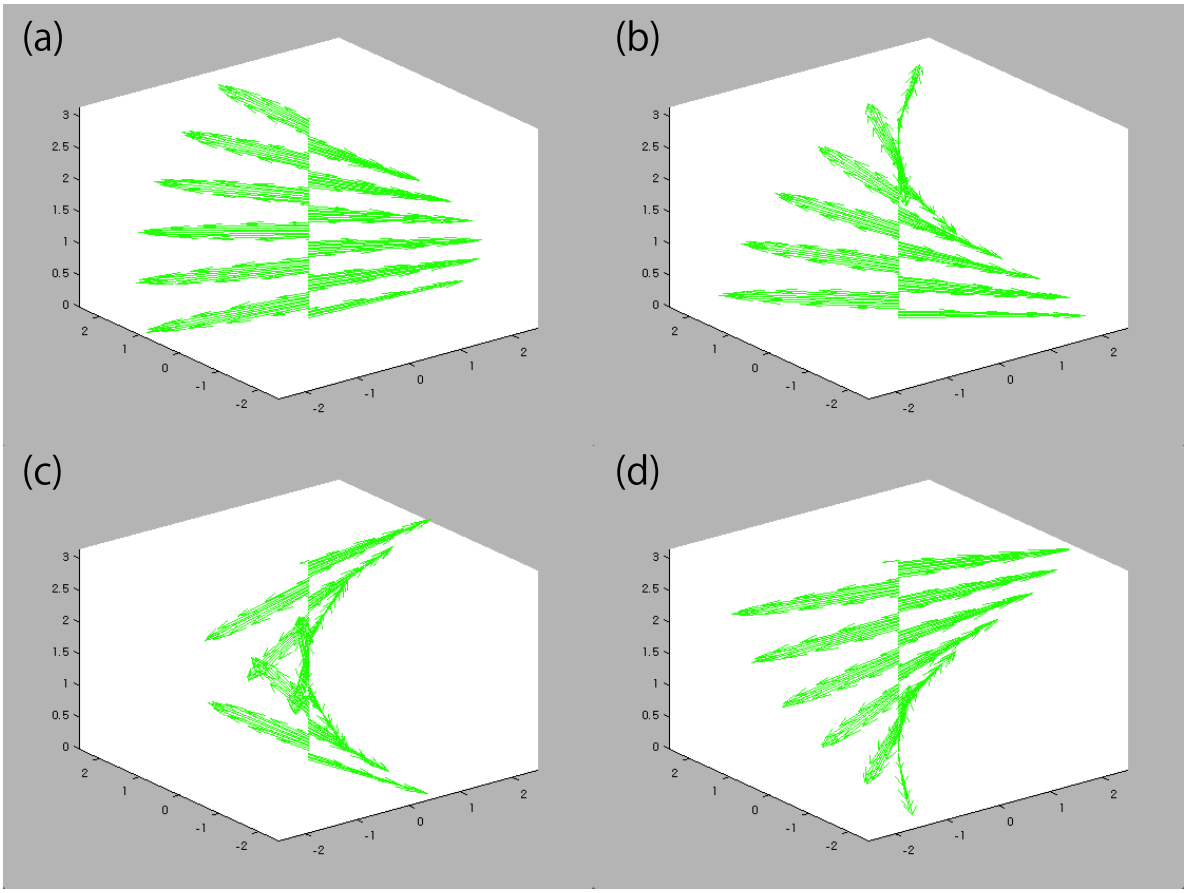

Fig. 2.5 Three-dimensional display of the horizontal velocity vectors of near-inertial beats along a fixed line in the vertical direction. Time variation is depicted in (a) → (b) → (c) → (d).

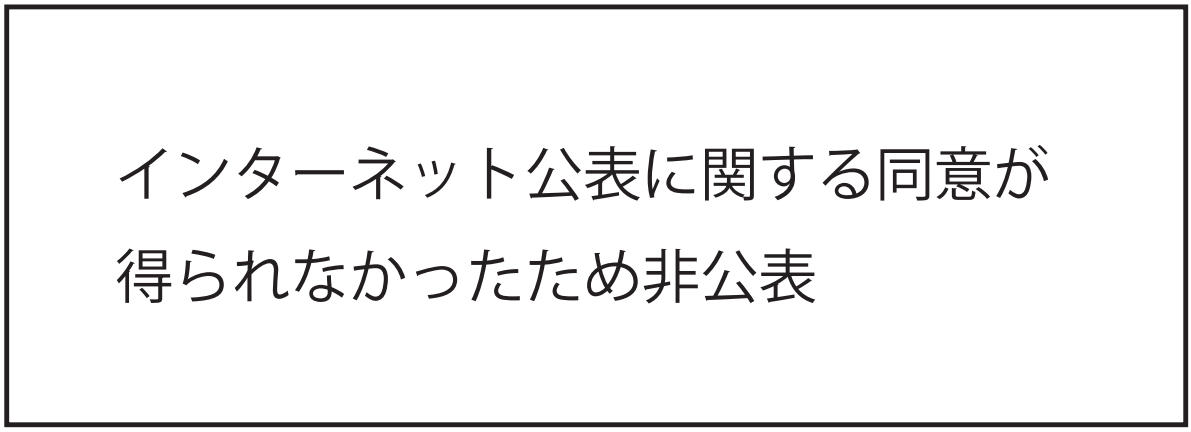

Fig. 2.6 Time variation of a baroclinic tidal flow (blue arrows) with 12-hour period and the near-inertial beats (green arrows) with 24-hour period both rotating in a horizontal plane. At 0H and 12H, the inertial beats are along the convergence direction of the background flow, so the acceleration occurs by the effect of convergence. At 3H, 9H, 15H, and 21H, the inertial beats obliquely cross the background shear layer, so the acceleration occurs by the effect of shear.

Chapter 3

Unified view on parametric instability

本章については、5 年以内に雑誌等で刊行予定のため、非公開。

Chapter 4

Attenuation rates of baroclinic tides

本章については、5 年以内に雑誌等で刊行予定のため、非公開。

Chapter 5

General conclusions

In this thesis, qualitative and quantitative aspects of nonlinear interactions among the oceanic internal waves, one of main processes for tidal dissipation in the ocean interior, are investigated. This chapter summarizes the main results obtained in each chapter and also in appendix. After that, their implication and possible future works are discussed.

5.1 Summary

In Chapter 2, the quantitative aspect of parametric subharmonic instability (PSI), the most significant phenomenon among resonant interactions in the ocean, is investigated without adhering to a strict mathematical formula. The visual image of PSI is offered using basic concepts, including *beats* and *parametric excitation*. Near the latitudes where half the tidal frequency coincides with the local inertial frequency, PSI is defined as a kind of parametric instability where *two disturbance waves propagating in opposite directions compose beats of velocity vectors locked with the phase of background waves resulting in successive advection of background momentum causing self-acceleration of disturbances*. An important implication is that the most effective interactions occur in some specific locations where horizontal velocities of both baroclinic tides and disturbance waves take their maximum values. This

finding offers a good perspective to detect the vertical distribution of energy dissipation rates, as will be discussed in Chapter 4.

In the following chapters, nonlinear interactions are quantitatively discussed from the view point of statistical mechanics. In Chapter 3, energy growth of disturbances in quasi-periodic waves is investigated. A nonlinear eigenvalue problem is systematically introduced using a temporal integro-differential equation and its approximate solution is derived as

$$\lambda = \frac{-\mu + \sqrt{\mu^2 + 4CE_B}}{2} \tag{5.1}$$

(written again from (3.64)), where μ, E_B are the spectral width and the energy density of the background wave and C is some constant. Conventional results which come from two approaches, called *dynamic* and *kinetic* theories, are unified in this formula. It is pointed out that μ is a new parameter which has been overlooked in the past numerical studies.

In the derivation of (5.1), it is also found that the classical kinetic theory is based not on the *random phase assumption* but on the *Markovian approximation*, which bankrupts when the time-variation of the energy spectrum is not slow enough compared to auto-correlation time of baroclinic tides. From this viewpoint, the kinetic equation is valid in steady states as far as the nonlinearity is sufficiently weak, which acts as the basis of the analysis in the following chapter.

In Chapter 4, the geographical features of the attenuation rates ν of baroclinic tides in a standard energy spectrum are calculated using new formulation of the kinetic equation. Remarkable enhancement of the attenuation rates is demonstrated near the critical latitudes of PSI, both for the diurnal and semidiurnal tidal constituents. Ocean depth and density stratification are additional factors which determine the local feature of interaction intensity among internal waves. In the subtropical region, shallow pycnocline in the eastern Pacific confines the wave structure of the lowest-mode baroclinic tides near the surface resulting in the rapid attenuation of them. Equivalent depth $\tilde{D}_m$ is a simple index which explains well the

variation of attenuation rates in a given latitude, with its scaling law $\nu \propto \tilde{D}_m^{-1/2}$ established in the lowest 5 modes.

The attenuation rate is further decomposed into the form of vertical integration as $\nu = \int \nu' dz$, integrand of which depends on the vertical structure functions, or velocity amplitudes, of interacting waves. The new index ν' takes large values in the upper ocean where horizontal velocities of each wave become maximum, as is inferred in Chapter 2. Those of the lowest-mode baroclinic tide are particularly concentrated near the surface, reflecting its characteristic vertical structure with its node located at subsurface. These results are expected to play a crucial role in the future study to compose the next generation ocean circulation models.

Although not explained in detail in the main text, this study is related to mathematical physics. In Appendix A to C, its theoretical fundamentals are lined up with minimal comments.

In Appendix A, as a preparation for the following part, general description of linear waves is made utilizing concepts of the pseudo-differential operator. Spatial differential operators characterizing the properties of waves in general media are transformed into symbol matrices. Introducing algebraic operations among symbol matrices, a general algorithm is arranged to separate intrinsic wave components from an original equation. After that, using the concepts of Wigner distribution function, quantum and classical Liouville equations in physical and wave vector space are systematically derived. The latter one appears in Chapter 4 as the energy transfer equation of baroclinic tides. A notable result in this section may be the assertion that energy flux is generally written as the product of energy density and intrinsic group velocity of it, like $\boldsymbol{F} = E\boldsymbol{c}_g$, even for inhomogeneous media, as far as some conditions (which are trivial for a rotating stratified fluid) are satisfied.

In Appendix B, formal statistical theories for nonlinear stochastic dynamical systems are systematically introduced, utilizing quantum field theory. The most fundamental one, called the Martin-Siggia-Rose formalism (MSR), is extended so as to be applicable to general sys-

tems with additive and multiplicative stochastic forces. After the bare vertex truncation, MSR is reduced to the direct interaction approximation (DIA) equation, which is expected to be valid even in strongly nonlinear systems. To derive the famous kinetic equation, additional two approximations are introduced: the weak interaction approximation (WIA) and the Markovian approximation (MA). It is pointed out that, even in weakly nonlinear systems, validity of MA is uncertain, which is the main issue in Chapter 3.

In a steady state, the kinetic equation is directly derived from WIA. Then, utilizing the methods in Appendix A, energy transfer equation (4.1) is derived with the specific expression of the attenuation term. It is also noted that, even in the case when WIA is not valid, another assumption of *dissipation fluctuation relationship* makes it possible to define the radiative transfer equation in the same form (4.1). In this case, the renormalized vertex and reaction function determine the property of the system, including the group velocity and the attenuation rate of each component. Therefore it may be said that the expression of attenuation rates derived from the kinetic equation is an approximate form of other *accurate* one. Along this sense, it is expected that the expression derived in this study will be replaced with more precise form.

In Appendix C, formal description in Appendix A,B are applied to oceanic internal motion. Starting from the variational principle, equations of motion are systematically introduced and transformed. Then we derive a kinetic equation applicable to vertical-low-mode internal waves, which is utilized for the calculation in Chapter 4.

As a summary, Fig. 5.1 shows a schematic flow chart of the contents in this thesis. Although several themes are discussed in this study, all the chapters are linked and indispensable to sustain the main conclusion: theory of statistical dynamics is an effective method for the study of nonlinear wave dynamics in the ocean and for the quantification of tidal dissipation. In the next and final section, we discuss the future study following this work.

5.2 Discussions and concluding remarks

Wave dynamics in the ocean is one of the biggest issues in physical oceanography. Even though innumerable studies have been done, global distribution of wave energy and its dissipation rate remain to be discovered. This is an obstacle to understand the global deep ocean circulation. From such view, results in this thesis should not be regarded as the goal, but as a step toward the final destination. In this section, conceivable studies following this thesis are discussed.

First, although the basic mechanism and quantification of PSI are clarified in Chapter 2 and 3, the author does not answer to a simple question;

> *Why are the disturbances most effectively excited near the latitudes where half the tidal frequency coincides with the local inertial frequency?*

This problem arises from numerical studies such as MacKinnon and Winters (2005) (hereafter MW05) who reported spontaneous enhancement of disturbance energy from sufficiently small homogeneous noise concentrated near the critical latitudes. The results of Chapter 4, where the background spectrum is prescribed, are not directly related to those of MW05. One phenomenological explanation for the latitudinal dependence of the resulting disturbances shown in MW05 is

> *Because the group velocity of subharmonic disturbances vanishes at the critical latitudes, accumulation of energy enlarges local instability.*

This plausible mechanism has not been considered in this thesis. A possible theoretical model reflecting this issue may be constructed by implementing flux terms into equation (3.54),

yielding

$$\begin{aligned}
&\frac{\partial n'}{\partial t} + \mu\nabla_x \cdot (\boldsymbol{c}_x n') + \mu\nabla_k \cdot (\boldsymbol{c}_k n') \\
=&\epsilon^2 \iint \int_{-\infty}^{0} \Big\{ R^\dagger(t-t')R(t-t')R^\dagger(t-t')|V|^2 N_B(\boldsymbol{k}_2) n'(\boldsymbol{k}_3, t')\delta(-\boldsymbol{k}+\boldsymbol{k}_2-\boldsymbol{k}_3) \\
&+ R^\dagger(t-t')R(t-t')R^\dagger(t-t')|V|^2 N_B(\boldsymbol{k}_2) n'(\boldsymbol{k}, t')\delta(-\boldsymbol{k}+\boldsymbol{k}_2-\boldsymbol{k}_3) \Big\} \\
&dt' d\boldsymbol{k}_2 d\boldsymbol{k}_3 + c.c.,
\end{aligned} \tag{5.2}$$

where all the variables are functions of $(\boldsymbol{x}, \boldsymbol{k})$. Stability analysis of (5.2) may be an effective approach, though it's not an easy way. Other studies about localized effects on parametric instability are seen in Karimi and Akylas (2014) and Bourget et al. (2014), which treat instabilities in tidal beams, although these studies may be still insufficient to completely resolve the problem. Any way, enhancement processes of disturbance waves are further to be investigated to detect the wave energy distribution in the ocean.

Second, assessment of wave-vortex interaction is an available task in near future. From theoretical consideration, in the weak interaction limit, the vortices act only as catalysts for waves. That is, vortex energy does not vary during the interaction with waves (Appendix C.5). In this situation, scattering rates of wave energy associated with wave-vortex interactions can be defined in the same way as attenuation rates associated with wave-wave interactions. Specific expression for the scattering rate is derived from the statistical theory. Given a spectrum of vortex energy, scattering rates of baroclinic tides will be calculated. Relative intensity of the scattering of baroclinic tides caused by vortices and its geography are significant concerns along with those for resonant interaction processes. Basic theoretical consideration and numerical studies of wave-vortex interaction have been done until now (Riley and Lelong, 2000; Ward and Dewar, 2010; Dunphy and Lamb, 2014; Zaron and Egbert, 2014). The statistical approach may become a new and effective method for this issue.

Wave scattering on ocean bottom topography is also a key factor for the energy loss of

baroclinic tides. However, steep bottom topography, which effectively scatters tidal energy, is difficult to be dealt with by weak-nonlinear theories. Because topography does not change with time, different from waves and vortices, deterministic approaches such as numerical simulation may be more suited to investigate the energy loss of baroclinic tides over topography than statistical methods.

It should be kept in mind that the energy lost from the tidal components does not necessarily dissipate locally, but may propagates as small-scale waves in both horizontal and vertical directions and will be dissipated through other dynamical processes. As has been mentioned in Section 1.3.2, the ray-tracing method will be useful to deal with this issue. It is expected that the kinetic equation and the ray-tracing method will be collaborated to investigate more thoroughly the spatial distribution of the mixing intensity associated with the dissipation of baroclinic tides.

Theoretical results in this thesis should be compared with those in direct observations. Above all, vertical distribution of interaction intensity between baroclinic tides and surrounding waves estimated in Chapter 4, which is a significant progress from the conventional studies, need to be compared with vertical profiler data of real ocean. Discussion in Chapter 3 is also aimed to be collaborated with observation studies. It has never been assessed so far how much the temporal variation of baroclinic tides affects the local energy spectrum of oceanic internal waves. The new formula (5.1) will act as a touchstone for this issue. Although the background spectrum is assumed to be a simple rational function in this thesis, the eigenvalue equation (3.54) is applicable to more general cases. Combination of line and smooth spectra may be a more proper model for the vicinity of generation sites of baroclinic tides. A two-peak spectrum in a narrow band will represent that of spring-neap tides. Although satellite observation in the last decades enables the global detection of vertical-low-mode baroclinic tides, temporal fluctuation of them induced by geostrophic eddies has been hardly analyzed because of the coarse temporal resolution of the satellite data (Zhao et al., 2012).

It is suggested that various approaches including numerical simulation, mooring observation and remote sensing need to be combined to discuss this issue.

One of the mid-term objectives of our study is to construct a practical method to estimate the energy dissipation rates of baroclinic tides in the ocean interior, and to implement them into general ocean models. Spherical distribution of the attenuation rates of baroclinic tides and the vertical distribution function of energy dissipation rates are typical ongoing parameters. A series of results obtained in Chapter 4 are prototypes of them and will be replaced with more reliable ones. Theoretical basis established in this thesis will become a milestone for the research that follows.

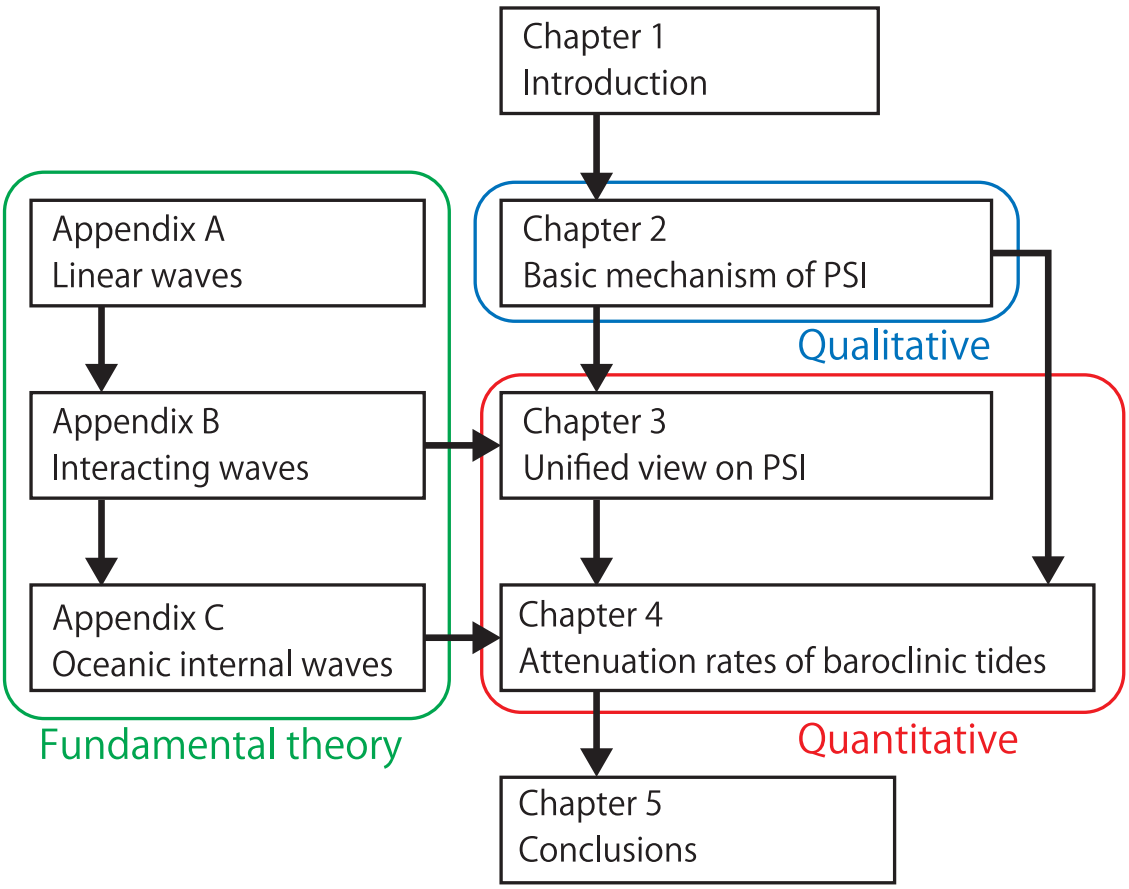

Fig. 5.1 A schematic flowchart for the contents in this thesis.

Appendix A

Linear waves in inhomogeneous media

本章については、5 年以内に雑誌等で刊行予定のため、非公開。

Appendix B

Statistical description for interacting waves

本章については、5 年以内に雑誌等で刊行予定のため、非公開。

Appendix C

Theoretical model of oceanic internal motion

本章については、5 年以内に雑誌等で刊行予定のため、非公開。

Appendix D

D.1 Specific expressions of functions in (3.67)

For simplicity, we choose $c_1 = 1, c_2 = -1$. After some analytical calculation, we obtain

$$\tilde{F}_0 = \frac{2r_2}{((c+1)\mu+\lambda)(r_2^2-\mu^2)} - \frac{2\mu}{((c+1)r_2+\lambda)(r_2^2-\mu^2)} \tag{D.1a}$$

$$\begin{aligned}\tilde{F}_2 = {} & \frac{8\mu}{((c+1)r_2+\lambda)^3(r_2^2-\mu^2)} - \frac{8r_2}{((c+1)\mu+\lambda)^3(r_2^2-\mu^2)} \\ & - \frac{8\mu r_2}{((c+1)r_2+\lambda)^2(r_2^2-\mu^2)^2} + \frac{8\mu r_2}{((c+1)\mu+\lambda)^2(r_2^2-\mu^2)^2} - \frac{8(c+1)\mu}{((c+1)r_2+\lambda)^3(r_2^2-\mu^2)} \\ & + \frac{2\lambda}{((c+1)^2\mu^2-\lambda^2)(r_2+\mu)^3} - \frac{2(c+1)^4\mu}{((c+1)^2\mu^2-\lambda^2)((c+1)r_2+\lambda)^3}\end{aligned} \tag{D.1b}$$

$$\tilde{G}_0 = \frac{2}{(c+1)\mu+\lambda} \tag{D.1c}$$

$$\tilde{G}_2 = -\frac{8}{((c+1)\mu+\lambda)^3} \tag{D.1d}$$

$$\tilde{H}_0 = \frac{2r_1}{((c-1)\mu+\lambda)(r_1^2-\mu^2)} - \frac{2\mu}{((c-1)r_1+\lambda)(r_1^2-\mu^2)} \tag{D.1e}$$

$$\begin{aligned}\tilde{H}_2 = {} & \frac{8\mu}{((c-1)r_1+\lambda)^3(r_1^2-\mu^2)} - \frac{8r_1}{((c-1)\mu+\lambda)^3(r_1^2-\mu^2)} \\ & + \frac{8\mu r_1}{((c-1)r_1+\lambda)^2(r_1^2-\mu^2)^2} - \frac{8\mu r_1}{((c-1)\mu+\lambda)^2(r_1^2-\mu^2)^2} + \frac{8(c-1)\mu}{((c-1)r_1+\lambda)^3(r_1^2-\mu^2)} \\ & + \frac{2\lambda}{((c-1)^2\mu^2-\lambda^2)(r_1+\mu)^3} - \frac{2(c-1)^4\mu}{((c-1)^2\mu^2-\lambda^2)((c-1)r_1+\lambda)^3}\end{aligned} \tag{D.1f}$$

$$\tilde{I}_0 = \frac{2}{(c-1)\mu+\lambda} \tag{D.1g}$$

$$\tilde{I}_2 = -\frac{8}{((c-1)\mu+\lambda)^3}. \tag{D.1h}$$

D.2 Solution of the inequality (4.7)

Solution of the inequality (4.7) is classified into five types, which are geometrically shown in Fig. D.1. In order to obtain the value of each endpoint of the integration interval, we need to solve a fourth-order algebraic equation

$$a_4 x^4 + a_3 x^3 + a_2 x^2 + a_1 x + a_0 = 0 \tag{D.2a}$$

$$a_4 \equiv (c_2^2 - c_3^2)^2 \tag{D.2b}$$

$$a_3 \equiv -4c_3^4\kappa_1 + 4c_2^2 c_3^2 \kappa_1 \tag{D.2c}$$

$$a_2 \equiv -2\omega_1^2 c_2^2 + 6c_3^4\kappa_1^2 - 2c_2^2 c_3^2 \kappa_1^2 - 2\omega_1^2 c_3^2 \tag{D.2d}$$

$$a_1 \equiv -4c_3^4\kappa_1^3 + 4\omega_1^2 c_3^2 \kappa_1 \tag{D.2e}$$

$$a_0 \equiv -4f^2\omega_1^2 + \omega_1^4 + c_3^4\kappa_1^4 - 2\omega_1^2 c_3^2 \kappa_1^2, \tag{D.2f}$$

with the condition of $|\omega_2(\kappa_2) - \omega_1| > f$. Letting the roots of (D.2) be x, endpoints are specified as $\kappa_2 = |x|$. In Chapter 4, this equation is numerically solved by the Bairstow method in quadruple precision. In this iterative method, initial values and the convergence condition are carefully arranged to prevent fatal numerical errors.

Because there is no upper limit of the solution in Fig. D.1(d), which occurs only in the case of $m_2 = m_3$, a proper truncation is taken.

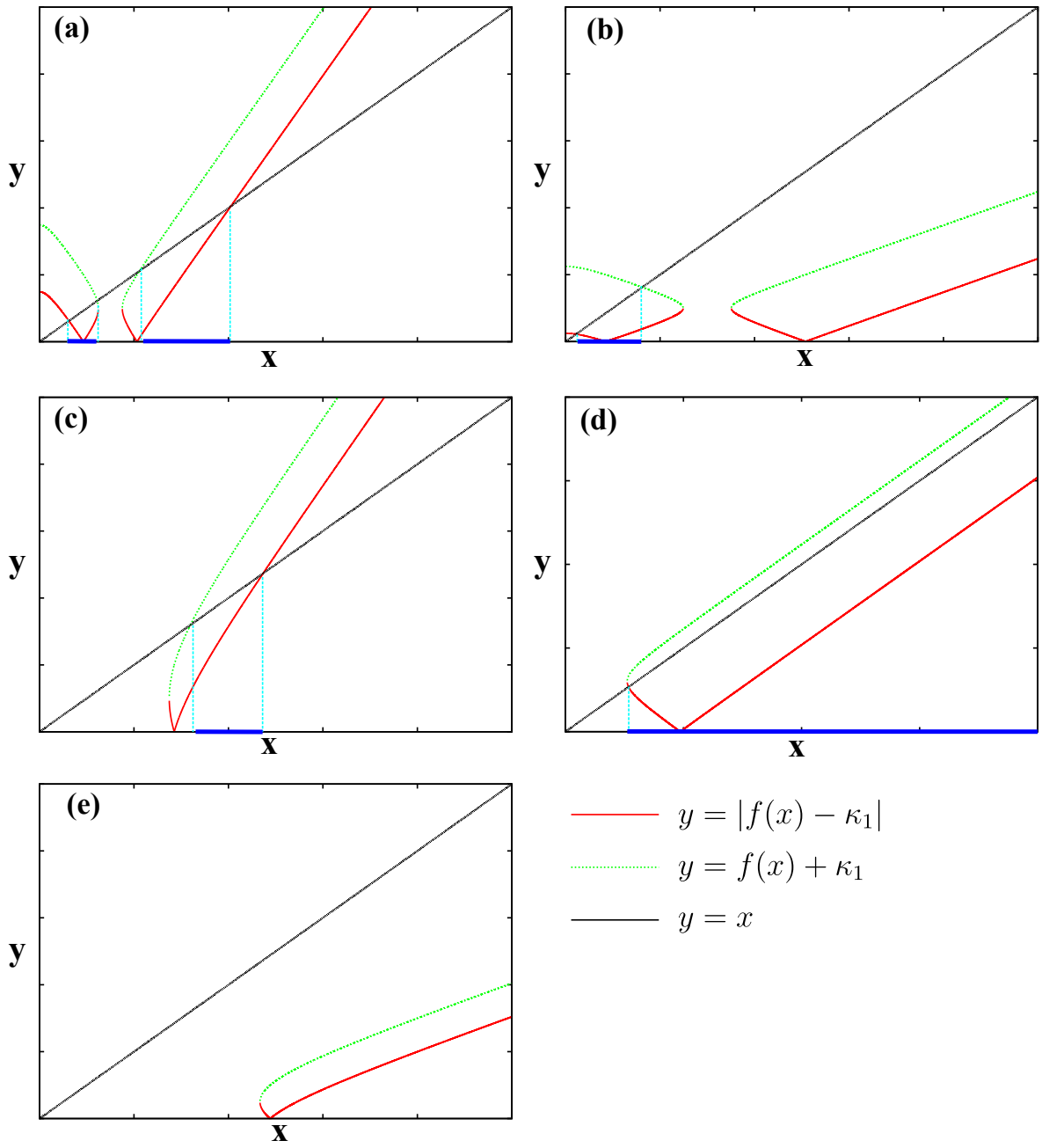

Fig. D.1 Geometric view of the inequality (4.7). Each term is depicted as a function of $x = \kappa_2$. Depending on the combination of (m_1, m_2, m_3), five types of situation occur. Blue lines in the horizontal axis show the intervals where the inequality is satisfied.

Acknowledgments

First and foremost, I would like to express my gratitude to my adviser, Prof. Toshiyuki Hibiya, for his many valuable suggestions and discussions over the past five years. This work would not have been possible without his continuous support.

My dissertation committee members Profs. Keita Iga, Ichiro Yasuda, Kaoru Sato, and Takuji Waseda provided many valuable comments and suggestions.

I am grateful to the very helpful members and ex-members of the Atmospheric and Oceanic Science Group, the University of Tokyo. Special thanks to Drs. Yoshihiro Niwa, Yuki Tanaka, Michio Watanabe, Taira Nagai, Takashi Ijichi, Yukio Masumoto, Tomoaki Tozuka, and Mr. Yuki Yasuda for their helpful suggestions and encouragement. Thanks are also due to Dr. Makoto Koike, Dr. Hiroaki Miura, Dr. Masashi Kohma, Dr. Kunihiro Aoki, Dr. Keiichi Hasunuma, Dr. Takenari Kinoshita, Dr. Takahito Kataoka, Mr. Shun Ohishi, Mr. Ryosuke Sibuya, Mr. Yuya Ozawa, Mr. Yang Wei, Mr. Tomoaki Takagi, Mr. Hajime Ishii, Mr. Yoko Yamagami, Ms. Tamaki Suematsu, Mr. Arata Amemiya, Mr. Soichiro Hirano, Mr. Ong Chiarui, Mr. Yuki Hayashi, Mr. Ryosuke Yasui, Ms. Anne Takahashi, Mr. Katsutoshi Fukuzawa, Mr. Shoichiro Kido, Mr. Yuichi Minamihara, Mr. Shuhei Matsugishi, Mr. Atsushi Yoshida, Ms. Emiri Kobori, and Mr. Koichi Sugiyama.

This study benefited from discussions with Drs. Akira Masuda, Naoki Hirose, Atsuhiko Isobe, Mitsuhiro Tanaka, Ryo Furue, Hiroyasu Hasumi, Yoshio Fukao, Michael Gregg, Hidenori Aiki, Takahiro Endoh, Shinichiro Kida, Naoki Furuichi, Daisuke Inazu, Akira Oka,

Eitaro Oka, Robin Robertson, and Naoto Yokoyama. My gratitude is also extended to Dr. Sunao Murashige, Dr. Daigo Yanagimoto, Dr. Genta Mizuta, Dr. Tsubasa Kodaira, Dr. Shota Katsura, Dr. Hidetaka Houtani, Dr. Hatsumi Nishikawa, Dr. Haruka Nakako, Mr. Hidetaka Kobayashi, Mr. Sam Sherriff-Tadano, Mr. Takashi Obase, Mr. Satoru Okajima, Mr. Yuichi Iwanaka, Mr. Masatoshi Miyamoto, Mr. Yasutaka Goto, Mr. Wataru Fujimto, Ms. Chorong Lee, Mr. Daiki Ito, Mr. Yasuhide Kobayashi, and Ms. Mio Terada.

Part of this study was supported by the Research Fellowship of the Japan Society for the Promotion of Science (JSPS). Numerical calculations were carried out on the Fujitsu PRIMEHPC FX10 System (Oakleaf-FX) in the Information Technology Center, the University of Tokyo. Part of algebraic and analytical calculation was done using Maxima. Figures were produced by The Grid Analysis and Display System (GrADS), MATLAB and Gnuplot.

Finally, I cannot fully express my gratitude to my family and friends for their support and encouragement.

Bibliography

Alber, I. E., 1978: The effects of randomness on the stability of two-dimensional surface wavetrains. *Proceedings of the Royal Society of London A: Mathematical, Physical and Engineering Sciences*, **363 (1715)**, 525–546, doi:10.1098/rspa.1978.0181.

Alford, M. H. and Z. Zhao, 2007: Global patterns of low-mode internal-wave propagation. part I: Energy and energy flux. *Journal of Physical Oceanography*, **37 (7)**, 1829–1848, doi:10.1175/JPO3085.1.

Altland, A. and B. Simons, 2010: *Condensed Matter Field Theory*. Cambridge books online, Cambridge University Press.

Amante, C. and B. W. Eakins, 2009: ETOPO1 Global Relief Model converted to PanMap layer format. PANGAEA, doi:10.1594/PANGAEA.769615.

Annenkov, S. Y. and V. I. Shrira, 2006: Role of non-resonant interactions in the evolution of nonlinear random water wave fields. *Journal of Fluid Mechanics*, **561**, 181–207, doi:10.1017/S0022112006000632.

Annenkov, S. Y. and V. I. Shrira, 2015: Modelling the impact of squall on wind waves with the generalized kinetic equation. *Journal of Physical Oceanography*, **45 (3)**, 807–812, doi:10.1175/JPO-D-14-0182.1.

Bender, C. and S. Orszag, 1999: *Advanced Mathematical Methods for Scientists and Engineers I: Asymptotic Methods and Perturbation Theory*. Advanced Mathematical Methods for Scientists and Engineers, Springer.

Benjamin, T. B. and J. E. Feir, 1967: The disintegration of wave trains on deep water. Part 1. Theory. *Journal of Fluid Mechanics*, **27**, 417–430, doi:10.1017/S002211206700045X.

Berera, A., M. Salewski, and W. D. McComb, 2013: Eulerian field-theoretic closure formalisms for fluid turbulence. *Phys. Rev. E*, **87**, 013 007, doi:10.1103/PhysRevE.87.013007.

Bokhove, O., 2000: On hydrostatic flows in isentropic coordinates. *Journal of Fluid Mechanics*, **402**, 291–310.

Bokhove, O., 2002a: Balanced models in geophysical fluid dynamics: Hamiltonian formulation, constraints and formal stability. *Large-Scale Atmosphere-Ocean Dynamics*, J. Norbury and I. Roulstone, Eds., Cambridge University Press, Cambridge, 1–63.

Bokhove, O., 2002b: Eulerian variational principles for stratified hydrostatic equations. *Journal of the Atmospheric Sciences*, **59 (9)**, 1619–1628, doi:10.1175/1520-0469(2002)059⟨1619:EVPFSH⟩2.0.CO;2.

Bourget, B., H. Scolan, T. Dauxois, M. L. Bars, P. Odier, and S. Joubaud, 2014: Finite-size effects in parametric subharmonic instability. *Journal of Fluid Mechanics*, **759**, 739–750, doi:10.1017/jfm.2014.550.

Bryan, F., 1987: Parameter sensitivity of primitive equation ocean general circulation models. *Journal of Physical Oceanography*, **17 (7)**, 970–985, doi:10.1175/1520-0485(1987)017⟨0970:PSOPEO⟩2.0.CO;2.

Carnevale, G. F. and J. S. Frederiksen, 1983: A statistical dynamical theory of strongly nonlinear internal gravity waves. *Geophysical & Astrophysical Fluid Dynamics*, **23 (3)**, 175–207, doi:10.1080/03091928308209042.

Chen, L. Y., N. Goldenfeld, and Y. Oono, 1994: Renormalization group theory for global asymptotic analysis. *Phys. Rev. Lett.*, **73**, 1311–1315, doi:10.1103/PhysRevLett.73.1311.

Chen, L.-Y., N. Goldenfeld, and Y. Oono, 1996: The Renormalization group and singular perturbations: Multiple scales, boundary layers and reductive perturbation theory. *Phys. Rev.*, **E54**, 376–394, doi:10.1103/PhysRevE.54.376.

Cohen, L., 2012: *The Weyl Operator and its Generalization*. Pseudo-Differential Operators, Springer Basel.

de Lavergne, C., G. Madec, J. L. Sommer, A. J. G. Nurser, and A. C. N. Garabato, 2016: The impact of a variable mixing efficiency on the abyssal overturning. *Journal of Physical Oceanography*, **46 (2)**, 663–681, doi:10.1175/JPO-D-14-0259.1.

Dewitt, R. J. and J. Wright, 1982: Self-consistent effective-medium theory of random internal waves. *Journal of Fluid Mechanics*, **115**, 283–302, doi:10.1017/S0022112082000755.

Dewitt, R. J. and J. Wright, 1984: Self-consistent effective-medium parameters for oceanic internal waves. *Journal of Fluid Mechanics*, **146**, 253–270, doi:10.1017/S0022112084001841.

Dunphy, M. and K. G. Lamb, 2014: Focusing and vertical mode scattering of the first mode internal tide by mesoscale eddy interaction. *Journal of Geophysical Research: Oceans*, **119 (1)**, 523–536, doi:10.1002/2013JC009293.

Eden, C., L. Czeschel, and D. Olbers, 2014: Toward energetically consistent ocean models. *Journal of Physical Oceanography*, **44 (12)**, 3160–3184, doi:10.1175/JPO-D-13-0260.1.

Eden, C. and D. Olbers, 2014: An energy compartment model for propagation, nonlinear interaction, and dissipation of internal gravity waves. *Journal of Physical Oceanography*, **44 (8)**, 2093–2106, doi:10.1175/JPO-D-13-0224.1.

Floris, C., 2012: Stochastic stability of damped Mathieu oscillator parametrically excited by a Gaussian noise. *Mathematical Problems in Engineering*, **2012**, 1 – 18.

Fukagawa, H. and Y. Fujitani, 2012: A variational principle for dissipative fluid dynamics. *Progress of Theoretical Physics*, **127 (5)**, 921–935, doi:10.1143/PTP.127.921.

Furuichi, N., T. Hibiya, and Y. Niwa, 2005: Bispectral analysis of energy transfer within the two-dimensional oceanic internal wave field. *Journal of Physical Oceanography*, **35 (11)**, 2104–2109, doi:10.1175/JPO2816.1.

Furuichi, N., T. Hibiya, and Y. Niwa, 2008: Model-predicted distribution of wind-induced

internal wave energy in the world's oceans. *Journal of Geophysical Research: Oceans*, **113 (C9)**, doi:10.1029/2008JC004768, c09034.

Garrett, C., 2003: Internal tides and ocean mixing. *Science*, **301 (5641)**, 1858–1859, doi:10.1126/science.1090002.

Garrett, C. and E. Kunze, 2007: Internal tide generation in the deep ocean. *Annual Review of Fluid Mechanics*, **39 (1)**, 57–87, doi:10.1146/annurev.fluid.39.050905.110227.

Garrett, C. and W. Munk, 1972: Space-time scales of internal waves. *Geophysical Fluid Dynamics*, **3 (1)**, 225–264, doi:10.1080/03091927208236082.

Garrett, C. and W. Munk, 1975: Space-time scales of internal waves: A progress report. *Journal of Geophysical Research*, **80 (3)**, 291–297, doi:10.1029/JC080i003p00291.

Gayen, B. and S. Sarkar, 2013: Degradation of an internal wave beam by parametric subharmonic instability in an upper ocean pycnocline. *Journal of Geophysical Research: Oceans*, **118 (9)**, 4689–4698, doi:10.1002/jgrc.20321.

Gérard, P., P. A. Markowich, N. J. Mauser, and F. Poupaud, 1997: Homogenization limits and Wigner transforms. *Communications on Pure and Applied Mathematics*, **50 (4)**, 323–379, doi:10.1002/(SICI)1097-0312(199704)50:4⟨323::AID-CPA4⟩3.0.CO;2-C.

Gill, A., 1982: *Atmosphere-Ocean Dynamics*. International Geophysics, Elsevier Science.

Goto, S. and S. Kida, 1998: Direct-interaction approximation and Reynolds-number reversed expansion for a dynamical system. *Physica D: Nonlinear Phenomena*, **117 (1)**, 191 – 214, doi:10.1016/S0167-2789(97)00314-X.

Gregg, M. C., 1989: Scaling turbulent dissipation in the thermocline. *Journal of Geophysical Research: Oceans*, **94 (C7)**, 9686–9698, doi:10.1029/JC094iC07p09686.

Hasselmann, K., 1962: On the non-linear energy transfer in a gravity-wave spectrum. Part 1. General theory. *Journal of Fluid Mechanics*, **12**, 481–500, doi:10.1017/S0022112062000373.

Hasselmann, K., 1966: Feynman diagrams and interaction rules of wave-wave scattering

processes. *Reviews of Geophysics*, **4 (1)**, 1–32, doi:10.1029/RG004i001p00001.

Hasselmann, K., 1967: A criterion for nonlinear wave stability. *Fluid Mech.*, **30**.

Hasselmann, K. and P. G. Saffman, 1967: Nonlinear interactions treated by the methods of theoretical physics (with application to the generation of waves by wind) [and discussion]. *Proceedings of the Royal Society of London A: Mathematical, Physical and Engineering Sciences*, **299 (1456)**, 77–103, doi:10.1098/rspa.1967.0124.

Hazewinkel, J. and K. B. Winters, 2011: PSI of the internal tide on a β plane: Flux divergence and near-inertial wave propagation. *Journal of Physical Oceanography*, **41 (9)**, 1673–1682, doi:10.1175/2011JPO4605.1.

Henyey, F. S., 1983: Hamiltonian description of stratified fluid dynamics. *Physics of Fluids*, **26 (1)**, 40–47, doi:10.1063/1.863981.

Henyey, F. S., J. Wright, and S. M. Flatt, 1986: Energy and action flow through the internal wave field: An eikonal approach. *Journal of Geophysical Research: Oceans*, **91 (C7)**, 8487–8495, doi:10.1029/JC091iC07p08487.

Hibiya, T., N. Furuichi, and R. Robertson, 2012: Assessment of fine-scale parameterizations of turbulent dissipation rates near mixing hotspots in the deep ocean. *Geophysical Research Letters*, **39 (24)**, doi:10.1029/2012GL054068, l24601.

Hibiya, T. and M. Nagasawa, 2004: Latitudinal dependence of diapycnal diffusivity in the thermocline estimated using a finescale parameterization. *Geophysical Research Letters*, **31 (1)**, doi:10.1029/2003GL017998, l01301.

Hibiya, T., M. Nagasawa, and Y. Niwa, 2002: Nonlinear energy transfer within the oceanic internal wave spectrum at mid and high latitudes. *Journal of Geophysical Research: Oceans*, **107 (C11)**, 28–1–28–8, doi:10.1029/2001JC001210, 3207.

Hibiya, T., M. Nagasawa, and Y. Niwa, 2006: Global mapping of diapycnal diffusivity in the deep ocean based on the results of expendable current profiler (XCP) surveys. *Geophysical Research Letters*, **33 (3)**, doi:10.1029/2005GL025218, l03611.

Hibiya, T., M. Nagasawa, and Y. Niwa, 2007: Latitudinal dependence of diapycnal diffusivity in the thermocline observed using a microstructure profiler. *Geophysical Research Letters*, **34 (24)**, doi:10.1029/2007GL032323, l24602.

Hibiya, T., Y. Niwa, and K. Fujiwara, 1998: Numerical experiments of nonlinear energy transfer within the oceanic internal wave spectrum. *Journal of Geophysical Research: Oceans*, **103 (C9)**, 18 715–18 722, doi:10.1029/98JC01362.

Hibiya, T., Y. Niwa, K. Nakajima, and N. Suginohara, 1996: Direct numerical simulation of the roll-off range of internal wave shear spectra in the ocean. *Journal of Geophysical Research: Oceans*, **101 (C6)**, 14 123–14 129, doi:10.1029/96JC01001.

Holloway, G., 1980: Oceanic internal waves are not weak waves. *Journal of Physical Oceanography*, **10 (6)**, 906–914, doi:10.1175/1520-0485(1980)010⟨0906:OIWANW⟩2.0.CO;2.

Holloway, G., 1982: On interaction time scales of oceanic internal waves. *Journal of Physical Oceanography*, **12 (3)**, 293–296, doi:10.1175/1520-0485(1982)012⟨0293:OITSOO⟩2.0.CO;2.

Holm, D. D. and B. Long, 1989: Lyapunov stability of ideal stratified fluid equilibria in hydrostatic balance. *Nonlinearity*, **2 (1)**, 23.

Huang, R. X., 2009: *Ocean Circulation: Wind-Driven and Thermohaline Processes*. Cambridge University Press, Cambridge, doi:10.1017/CBO9780511812293.

Ijichi, T. and T. Hibiya, 2015: Frequency-based correction of finescale parameterization of turbulent dissipation in the deep ocean. *Journal of Atmospheric and Oceanic Technology*, **32 (8)**, 1526–1535, doi:10.1175/JTECH-D-15-0031.1.

Ijichi, T. and T. Hibiya, 2016: Eikonal calculations for energy transfer in the deep-ocean internal wave field near mixing hotspots. *Journal of Physical Oceanography, in press*, doi:10.1175/JPO-D-16-0093.1.

Janssen, P. A. E. M., 2003: Nonlinear four-wave interactions and freak waves. *Jour-*

nal of Physical Oceanography, **33 (4)**, 863–884, doi:10.1175/1520-0485(2003)33⟨863:NFIAFW⟩2.0.CO;2.

Jayne, S. R. and L. C. St. Laurent, 2001: Parameterizing tidal dissipation over rough topography. *Geophysical Research Letters*, **28 (5)**, 811–814, doi:10.1029/2000GL012044.

Karimi, H. H. and T. R. Akylas, 2014: Parametric subharmonic instability of internal waves: locally confined beams versus monochromatic wavetrains. *Journal of Fluid Mechanics*, **757**, 381–402, doi:10.1017/jfm.2014.509.

Kartashova, E., 2013: Time scales and structures of wave interaction exemplified with water waves. *EPL (Europhysics Letters)*, **102 (4)**, 44 005.

Kraichnan, R. H., 1959: The structure of isotropic turbulence at very high Reynolds numbers. *Journal of Fluid Mechanics*, **5**, 497–543, doi:10.1017/S0022112059000362.

Kubo, R., 1964: Wigner representation of quantum operators and its applications to electrons in a magnetic field. *Journal of the Physical Society of Japan*, **19 (11)**, 2127–2139, doi:10.1143/JPSJ.19.2127.

Kunze, E., E. Firing, J. M. Hummon, T. K. Chereskin, and A. M. Thurnherr, 2006: Global abyssal mixing inferred from lowered ADCP shear and CTD strain profiles. *Journal of Physical Oceanography*, **36 (8)**, 1553–1576, doi:10.1175/JPO2926.1.

Landau, L. and E. Lifshitz, 1976: *Mechanics*. Butterworth-Heinemann, Butterworth-Heinemann.

Locarnini, R. A., et al., 2013: *World Ocean Atlas 2013: Temperature*. No. 1 in NOAA atlas NESDIS.

Longuet-Higgins, M., 1964: On group velocity and energy flux in planetary wave motions. *Deep Sea Research and Oceanographic Abstracts*, **11 (1)**, 35 – 42, doi:10.1016/0011-7471(64)91080-0.

L'vov, V. S. and S. Nazarenko, 2010: Discrete and mesoscopic regimes of finite-size wave turbulence. *Phys. Rev. E*, **82**, 056 322, doi:10.1103/PhysRevE.82.056322.

Lvov, Y. and E. G. Tabak, 2004: A Hamiltonian formulation for long internal waves. *Physica D: Nonlinear Phenomena*, **195 (1-2)**, 106–122, doi:10.1016/j.physd.2004.03.010.

Lvov, Y. V., K. L. Polzin, and N. Yokoyama, 2012: Resonant and near-resonant internal wave interactions. *Journal of Physical Oceanography*, **42 (5)**, 669–691, doi:10.1175/2011JPO4129.1.

MacKinnon, J. A., M. H. Alford, O. Sun, R. Pinkel, Z. Zhao, and J. Klymak, 2013: Parametric subharmonic instability of the internal tide at 29° N. *Journal of Physical Oceanography*, **43 (1)**, 17–28, doi:10.1175/JPO-D-11-0108.1.

MacKinnon, J. A. and K. B. Winters, 2005: Subtropical catastrophe: Significant loss of low-mode tidal energy at 28.9°. *Geophysical Research Letters*, **32 (15)**, doi:10.1029/2005gl023376.

Martin, P. C., E. D. Siggia, and H. A. Rose, 1973: Statistical dynamics of classical systems. *Phys. Rev. A*, **8**, 423–437, doi:10.1103/PhysRevA.8.423.

McComas, C. H., 1977: Equilibrium mechanisms within the oceanic internal wave field. *Journal of Physical Oceanography*, **7 (6)**, 836–845, doi:10.1175/1520-0485(1977)007⟨0836:EMWTOI⟩2.0.CO;2.

McComas, C. H. and F. P. Bretherton, 1977: Resonant interaction of oceanic internal waves. *Journal of Geophysical Research*, **82 (9)**, 1397–1412, doi:10.1029/JC082i009p01397.

McComas, C. H. and P. Müller, 1981: Time scales of resonant interactions among oceanic internal waves. *Journal of Physical Oceanography*, **11 (2)**, 139–147, doi:10.1175/1520-0485(1981)011⟨0139:TSORIA⟩2.0.CO;2.

Medvedev, S. and V. Zeitlin, 2007: Turbulence of near-inertial waves in the continuously stratified fluid. *Physics Letters A*, **371 (3)**, 221 – 227, doi:10.1016/j.physleta.2007.08.014.

Meiss, J. D., N. Pomphrey, and K. M. Watson, 1979: Numerical analysis of weakly nonlinear wave turbulence. *Proceedings of the National Academy of Sciences*, **76 (5)**, 2109–2113.

Melet, A., S. Legg, and R. Hallberg, 2016: Climatic impacts of parameterized local and re-

mote tidal mixing. *Journal of Climate*, **29 (10)**, 3473–3500, doi:10.1175/JCLI-D-15-0153.1.

Morrison, P. J., 1998: Hamiltonian description of the ideal fluid. *Rev. Mod. Phys.*, **70**, 467–521, doi:10.1103/RevModPhys.70.467.

Müller, P., G. Holloway, F. Henyey, and N. Pomphrey, 1986: Nonlinear interactions among internal gravity waves. *Reviews of Geophysics*, **24 (3)**, 493–536, doi:10.1029/RG024i003p00493.

Munk, W., 1981: Internal waves and small-scale processes. *Evolution of Physical Oceanography*, W. B. A. and W. C., Eds., The MIT Press, chap. 9.

Munk, W. and C. Wunsch, 1998: Abyssal recipes II: energetics of tidal and wind mixing. *Deep Sea Research Part I: Oceanographic Research Papers*, **45 (12)**, 1977 – 2010, doi:10.1016/S0967-0637(98)00070-3.

Munk, W. H., 1966: Abyssal recipes. *Deep Sea Research and Oceanographic Abstracts*, **13**, 707–730, doi:10.1016/0011-7471(66)90602-4.

Nazarenko, S., 2011: *Wave Turbulence*. Lecture Notes in Physics, Springer.

Niwa, Y. and T. Hibiya, 2004: Three-dimensional numerical simulation of M_2 internal tides in the east china sea. *Journal of Geophysical Research: Oceans*, **109 (C4)**, doi:10.1029/2003JC001923, c04027.

Niwa, Y. and T. Hibiya, 2011: Estimation of baroclinic tide energy available for deep ocean mixing based on three-dimensional global numerical simulations. *Journal of Oceanography*, **67 (4)**, 493–502, doi:10.1007/s10872-011-0052-1.

Niwa, Y. and T. Hibiya, 2014: Generation of baroclinic tide energy in a global three-dimensional numerical model with different spatial grid resolutions. *Ocean Modelling*, **80**, 59 – 73, doi:10.1016/j.ocemod.2014.05.003.

Oka, A. and Y. Niwa, 2013: Pacific deep circulation and ventilation controlled by tidal mixing away from the sea bottom. *Nature Communications*, **4**, 2419, doi:10.1038/ncomms3419.

Olbers, D. and C. Eden, 2013: A global model for the diapycnal diffusivity induced by internal gravity waves. *Journal of Physical Oceanography*, **43 (8)**, 1759–1779, doi:10.1175/JPO-D-12-0207.1.

Olbers, D., J. Willebrand, and C. Eden, 2012: *Ocean Dynamics*. Springer Verlag Berlin, Berlin.

Olbers, D. J., 1976: Nonlinear energy transfer and the energy balance of the internal wave field in the deep ocean. *Journal of Fluid Mechanics*, **74**, 375–399, doi:10.1017/S0022112076001857.

Olbers, D. J., 1983: Models of the oceanic internal wave field. *Reviews of Geophysics*, **21 (7)**, 1567–1606, doi:10.1029/RG021i007p01567.

Olbers, D. J. and N. Pomphrey, 1981: Disqualifying two candidates for the energy balance of oceanic internal waves. *Journal of Physical Oceanography*, **11 (10)**, 1423–1425, doi:10.1175/1520-0485(1981)011⟨1423:DTCFTE⟩2.0.CO;2.

Osborn, T. R., 1980: Estimates of the local rate of vertical diffusion from dissipation measurements. *Journal of Physical Oceanography*, **10 (1)**, 83–89, doi:10.1175/1520-0485(1980)010⟨0083:EOTLRO⟩2.0.CO;2.

Pedlosky, J., 1979: *Geophysical fluid dynamics*. Springer Verlag, New York, includes index.

Peskin, M. E. and D. V. Schroeder, 1995: *An Introduction to Quantum Field Theory; 1995 ed.* Westview, Boulder, Colorado.

Polzin, K. L. and Y. V. Lvov, 2011: Toward regional characterizations of the oceanic internal wavefield. *Reviews of Geophysics*, **49 (4)**, doi:10.1029/2010RG000329, rG4003.

Polzin, K. L., J. M. Toole, and R. W. Schmitt, 1995: Finescale parameterizations of turbulent dissipation. *Journal of Physical Oceanography*, **25 (3)**, 306–328, doi:10.1175/1520-0485(1995)025⟨0306:FPOTD⟩2.0.CO;2.

Pomphrey, N., J. D. Meiss, and K. M. Watson, 1980: Description of nonlinear internal wave interactions using Langevin methods. *Journal of Geophysical Research: Oceans*, **85 (C2)**,

1085–1094, doi:10.1029/JC085iC02p01085.

Potapov, V. D., 2008: Stability of elastic systems under a stochastic parametric excitation. *Archive of Applied Mechanics*, **78 (11)**, 883–894, doi:10.1007/s00419-007-0196-z.

Qiu, B., S. Chen, and G. S. Carter, 2012: Time-varying parametric subharmonic instability from repeat CTD surveys in the northwestern Pacific Ocean. *Journal of Geophysical Research: Oceans*, **117 (C9)**, doi:10.1029/2012JC007882, c09012.

Ray, R. D. and E. D. Zaron, 2016: M_2 internal tides and their observed wavenumber spectra from satellite altimetry. *Journal of Physical Oceanography*, **46 (1)**, 3–22, doi:10.1175/JPO-D-15-0065.1.

Riley, J. J. and M.-P. Lelong, 2000: Fluid motions in the presence of strong stable stratification. *Annual Review of Fluid Mechanics*, **32 (1)**, 613–657, doi:10.1146/annurev.fluid.32.1.613.

Rong, H., G. Meng, X. Wang, W. Xu, and T. Fang, 2002: Invariant measures and Lyapunov exponents for stochastic Mathieu system. *Nonlinear Dynamics*, **30 (4)**, 313–321, doi:10.1023/A:1021208631414.

Ryzhik, L., G. Papanicolaou, and J. B. Keller, 1996: Transport equations for elastic and other waves in random media. *Wave Motion*, **24 (4)**, 327 – 370, doi:10.1016/S0165-2125(96)00021-2.

Sakurai, J. and J. Napolitano, 2011: *Modern Quantum Mechanics*. Addison-Wesley.

Salmon, R., 1998: *Lectures on Geophysical Fluid Dynamics*. Oxford University Press, USA.

Shepherd, T. G., 1990: Symmetries, conservation laws, and Hamiltonian structure in geophysical fluid dynamics. Elsevier, Advances in Geophysics, Vol. 32, 287 – 338, doi:10.1016/S0065-2687(08)60429-X.

Shepherd, T. G., 1993: A unified theory of available potential energy. *Atmosphere-Ocean*, **31 (1)**, 1–26, doi:10.1080/07055900.1993.9649460.

Shriver, J. F., B. K. Arbic, J. G. Richman, R. D. Ray, E. J. Metzger, A. J. Wallcraft, and

P. G. Timko, 2012: An evaluation of the barotropic and internal tides in a high-resolution global ocean circulation model. *Journal of Geophysical Research: Oceans*, **117 (C10)**, doi:10.1029/2012JC008170, c10024.

Simmons, H. L., 2008: Spectral modification and geographic redistribution of the semi-diurnal internal tide. *Ocean Modelling*, **21 (34)**, 126 – 138, doi:10.1016/j.ocemod.2008.01.002.

Simmons, H. L., S. R. Jayne, L. C. Laurent, and A. J. Weaver, 2004: Tidally driven mixing in a numerical model of the ocean general circulation. *Ocean Modelling*, **6 (34)**, 245 – 263, doi:10.1016/S1463-5003(03)00011-8.

Sonmor, L. J. and G. P. Klaassen, 1997: Toward a unified theory of gravity wave stability. *Journal of the Atmospheric Sciences*, **54 (22)**, 2655–2680, doi:10.1175/1520-0469(1997)054⟨2655:TAUTOG⟩2.0.CO;2.

St. Laurent, L. and C. Garrett, 2002: The role of internal tides in mixing the deep ocean. *Journal of Physical Oceanography*, **32 (10)**, 2882–2899, doi:10.1175/1520-0485(2002)032⟨2882:TROITI⟩2.0.CO;2.

St. Laurent, L. C., H. L. Simmons, and S. R. Jayne, 2002: Estimating tidally driven mixing in the deep ocean. *Geophysical Research Letters*, **29 (23)**, 21–1–21–4, doi:10.1029/2002GL015633, 2106.

St. Laurent, L. C., J. M. Toole, and R. W. Schmitt, 2001: Buoyancy forcing by turbulence above rough topography in the abyssal Brazil Basin*. *Journal of Physical Oceanography*, **31 (12)**, 3476–3495, doi:10.1175/1520-0485(2001)031⟨3476:BFBTAR⟩2.0.CO;2.

Tsujino, H., H. Hasumi, and N. Suginohara, 2000: Deep Pacific circulation controlled by vertical diffusivity at the lower thermocline depths. *Journal of Physical Oceanography*, **30 (11)**, 2853–2865, doi:10.1175/1520-0485(2001)031⟨2853:DPCCBV⟩2.0.CO;2.

Vallis, G. K., 2006: *Atmospheric and Oceanic Fluid Dynamics*. Cambridge University Press, Cambridge, U.K., 745 pp.

Ward, M. L. and W. K. Dewar, 2010: Scattering of gravity waves by potential vorticity in a shallow-water fluid. *Journal of Fluid Mechanics*, **663**, 478–506, doi:10.1017/S0022112010003721.

Waseda, T., T. Kinoshita, and H. Tamura, 2009: Evolution of a random directional wave and freak wave occurrence. *Journal of Physical Oceanography*, **39 (3)**, 621–639, doi:10.1175/2008JPO4031.1.

Yokoyama, N., 2011: Wave turbulent statistics in non-weak wave turbulence. *Phys. Lett. A*, **375**, 4280–4287.

Young, W. R., Y.-K. Tsang, and N. J. Balmforth, 2008: Near-inertial parametric subharmonic instability. *Journal of Fluid Mechanics*, **607**, 25–49, doi:10.1017/S0022112008001742.

Zakharov, V. E., A. O. Korotkevich, A. N. Pushkarev, and A. I. Dyachenko, 2005: Mesoscopic wave turbulence. *Journal of Experimental and Theoretical Physics Letters*, **82 (8)**, 487–491, doi:10.1134/1.2150867.

Zakharov, V. E., V. S. L'vov, and G. Falkovich, 1992: *Kolmogorov Spectra of Turbulence I - Wave Turbulence*. Springer.

Zaron, E. D. and G. D. Egbert, 2014: Time-variable refraction of the internal tide at the Hawaiian Ridge. *Journal of Physical Oceanography*, **44 (2)**, 538–557, doi:10.1175/JPO-D-12-0238.1.

Zhao, Z., M. H. Alford, and J. B. Girton, 2012: Mapping low-mode internal tides from multisatellite altimetry. *Oceanography*, **25**.

Zhao, Z., M. H. Alford, J. B. Girton, L. Rainville, and H. L. Simmons, 2016: Global observations of open-ocean mode-1 M_2 internal tides. *Journal of Physical Oceanography*, **46 (6)**, 1657–1684, doi:10.1175/JPO-D-15-0105.1.

Zweng, M., et al., 2013: *World Ocean Atlas 2013: Salinity*. No. 2 in NOAA atlas NESDIS.